

Loss of ULK1 increases RPS6KB1-NCOR1 repression of NR1H/LXR-mediated *Scd1* transcription and augments lipotoxicity in hepatic cells

Rohit Anthony Sinha^a, Brijesh K. Singh^a, Jin Zhou^a, Sherwin Xie^a, Benjamin L. Farah^a, Ronny Lesmana^{a,b}, Kenji Ohba^a, Madhulika Tripathi^c, Sujoy Ghosh^a, Anthony N. Hollenberg^d, and Paul M. Yen^a

^aLaboratory of Hormonal Regulation, Cardiovascular and Metabolic Disorders Program, Duke-NUS Graduate Medical School, Singapore; ^bDepartment of Physiology, Universitas Padjadjaran, Bandung, Indonesia; ^cStroke Trial Unit, National Neuroscience Institute Singapore, Singapore; ^dDivision of Endocrinology, Diabetes and Metabolism, Beth Israel Deaconess Medical Center and Harvard Medical School, Boston, MA USA

ABSTRACT

Lipotoxicity caused by saturated fatty acids (SFAs) induces tissue damage and inflammation in metabolic disorders. SCD1 (stearoyl-coenzyme A desaturase 1) converts SFAs to mono-unsaturated fatty acids (MUFAs) that are incorporated into triglycerides and stored in lipid droplets. SCD1 thus helps protect hepatocytes from lipotoxicity and its reduced expression is associated with increased lipotoxic injury in cultured hepatic cells and mouse models. To further understand the role of SCD1 in lipotoxicity, we examined the regulation of *Scd1* in hepatic cells treated with palmitate, and found that NR1H/LXR (nuclear receptor subfamily 1 group H) ligand, GW3965, induced *Scd1* expression and lipid droplet formation to improve cell survival. Surprisingly, ULK1/ATG1 (unc-51 like kinase) played a critical role in protecting hepatic cells from SFA-induced lipotoxicity via a novel mechanism that did not involve macroautophagy/autophagy. Specific loss of *Ulk1* blocked the induction of *Scd1* gene transcription by GW3965, decreased lipid droplet formation, and increased apoptosis in hepatic cells exposed to palmitate. Knockdown of ULK1 increased RPS6KB1 (ribosomal protein S6 kinase, polypeptide 1) signaling that, in turn, induced NCOR1 (nuclear receptor co-repressor 1) nuclear uptake, interaction with NR1H/LXR, and recruitment to the *Scd1* promoter. These events abrogated the stimulation of *Scd1* gene expression by GW3965, and increased lipotoxicity in hepatic cells. In summary, we have identified a novel autophagy-independent role of ULK1 that regulates NR1H/LXR signaling, *Scd1* expression, and intracellular lipid homeostasis in hepatic cells exposed to a lipotoxic environment.

ARTICLE HISTORY

Received 20 November 2015
Revised 23 August 2016
Accepted 7 September 2016

KEYWORDS

autophagy; lipid droplets; lipotoxicity; LXR; NASH; NCOR1; RPS6KB1; SCD1; ULK1

Introduction


Lipotoxicity is a characteristic feature of metabolic syndrome that results from the overaccumulation of SFAs and their toxic metabolites in nonadipose tissues such as liver, kidneys, pancreas, heart and skeletal muscle. This overaccumulation leads to metabolic changes and tissue damage that can lead to disorders such as diabetes and nonalcoholic steatohepatitis (NASH).^{1–7} At the cellular level, SFAs induce lipotoxicity by increasing ER stress and apoptosis.^{2,8} To counteract lipotoxicity, cells employ 2 major methods: β -oxidation of FAs in mitochondria and/or storage of FAs within neutral LD(s) (lipid droplets).^{9–11} Failure of either of these processes enables FAs to be converted to toxic lipid intermediates such as diacylglycerol, ceramides and fatty acyl-CoAs that can impair cellular function and decrease cell viability.^{7,12} The process of shuttling SFAs into neutral LDs requires the action of SCD1, an endoplasmic reticulum iron-containing microsomal enzyme required for endogenous formation of MUFAs from SFAs substrates.¹³ Recent in vivo studies have shown that SCD1 is a critical determinant of lipotoxicity in liver, pancreas, heart and muscles

that are challenged with lipid overload.^{14–19} *Scd1* mRNA expression is regulated by exercise, intracellular concentrations of SFAs and cholesterol, as well as by ligands for nuclear receptors such as NR1H/LXRs.²⁰ Ligand-bound NR1H/LXRs increase the transcription of *Scd1* gene by directly binding to its upstream promoter.²¹ In this regard, NR1H/LXR ligands have been shown to reduce lipotoxicity in human arterial endothelial cells by increasing *Scd1*.¹⁶

Autophagy is a conserved cellular catabolic process that provides energy during starvation. In autophagy, a set of autophagy gene products works in concert to promote autophagic flux through key processes such as autophagosome biogenesis, lysosomal fusion, and cargo degradation.²² The role of autophagy in lipotoxicity is unclear as conflicting results have been reported. Autophagy commonly provides protection against lipotoxicity induced by SFAs;^{23–25} however, paradoxically it also can worsen the effects of lipotoxicity in certain cell types.^{26,27} Similarly, there currently is debate over the effects of autophagy on cellular lipid metabolism. In this connection, autophagy has been shown to both degrade^{28–31} and assemble

CONTACT Rohit Anthony Sinha  rohit.sinha@duke-nus.edu.sg; anthony.rohit@gmail.com; Paul M. Yen  paul.yen@duke-nus.edu.sg  Laboratory of Hormonal Regulation, Cardiovascular and Metabolic Disorders Program, Duke-NUS Graduate Medical School, 8 College Road, Singapore - 169857.

Color versions of one or more of the figures in the article can be found online at www.tandfonline.com/kaup.

 Supplemental data for this article can be accessed on the publisher's website.

© 2017 Rohit Anthony Sinha, Brijesh K. Singh, Jin Zhou, Sherwin Xie, Benjamin L. Farah, Ronny Lesmana, Kenji Ohba, Madhulika Tripathi, Sujoy Ghosh, Anthony N. Hollenberg, and Paul M. Yen. Published with license by Taylor & Francis.

This is an Open Access article distributed under the terms of the Creative Commons Attribution-Non-Commercial License (<http://creativecommons.org/licenses/by-nc/3.0/>), which permits unrestricted non-commercial use, distribution, and reproduction in any medium, provided the original work is properly cited. The moral rights of the named author(s) have been asserted.

lipid droplets.³²⁻³⁵ Furthermore, the role(s) of individual autophagy-related (ATG) proteins in cellular lipid metabolism during lipotoxicity is not well understood.

ULK1/ATG1 is the only kinase within the ATG family of proteins, and is an important component of the AMP-activated protein kinase (AMPK) and MTOR kinase pathways to sense and regulate cellular energy balance.³⁶⁻³⁹ Although ULK1 is critical in mediating starvation-induced general autophagy, it is also an important regulator of selective types of autophagy such as mitophagy.^{40,41} Interestingly, several nonautophagic functions of ULK1 have been recently discovered,⁴²⁻⁴⁵ suggesting that it may have a broader role in cellular signaling in addition to autophagy.

In this manuscript, we describe for the first time that ULK1 has an autophagy-independent role in cellular lipid homeostasis and lipotoxicity by virtue of its regulation of *Scd1* expression. Silencing *Ulk1* in hepatic cells leads to phosphorylation of RPS6KB1, intranuclear localization of the corepressor NCOR1, and repression of NR1H/LXR-mediated transcription of the *Scd1* gene. This, in turn, leads to decreased lipid droplet formation and increased lipotoxicity upon palmitic acid (PA) exposure. Thus, our results show a novel and important role of ULK1 in hepatocellular lipid partitioning and homeostasis.

Results

NR1H/LXR ligand, GW3965 protects hepatic cells from lipotoxicity by inducing *Scd1* expression, and lipid droplet formation

There are 2 isoforms of NR1H/LXRs, NR1H3/LXR α and NR1H2/LXR β , that are activated by oxysterols;⁴⁶ however, synthetic ligands such as GW3965 also can bind to NR1H/LXRs with high selectivity and potency in vitro. The efficacy of this NR1H/LXR agonist in preventing lipotoxicity by SFAs in hepatic cells was examined in AML-12 cells (immortalized adult mouse hepatocytes) exposed to palmitic acid. Our results showed that GW3965 significantly inhibited PA-induced cell death (Fig. 1A). The nature of PA-induced cell death was apoptotic and was confirmed by analysis of the sub-G₁ peak (Fig. 1B), cleavage of CASP3 (Fig. 1C, D), TUNEL staining (Fig. S1A), and electron microscopy (Fig. S1B). Other known cellular effects of PA toxicity such as lipid peroxidation and ER stress also were rescued by GW3965 (Fig. S2A, B). In parallel with these protective effects, GW3965 increased lipid droplet (LD) formation in PA-treated cells when observed with a lipophilic dye, BODIPY 493/503 (Fig. 1E). GW3965 also induced mRNA expression of the lipogenic genes *Scd1* and *Fasn* in the presence of PA (Fig. 1F).

Using specific knockdown of NR1H/LXR-induced genes such as *Fasn* and *Scd1*, we inferred that SCD1 activity was the major regulator of NR1H/LXR-induced LD accumulation in response to PA (Fig. S3A, B). These results were further supported by the relatively greater accumulation of LD in response to oleate-loading compared to PA-loading (Fig. S3A), suggesting that unsaturated fatty acids are preferred over saturated ones in the formation of LDs. In this connection, SCD1 has been shown to protect against lipotoxicity in other cell types.¹⁷ In order to confirm that SCD1

expression was necessary for GW3965-mediated protection, we knocked down *Scd1* by siRNA or used a SCD1 enzymatic inhibitor in cells that were treated with PA in the absence or presence of GW3965. Our results showed that both gene silencing of *Scd1* and its pharmacological inhibition completely ablated the anti-apoptotic effect by GW3965 in PA-treated cells (Fig. 2A, B and Fig. S4A, B). Additionally, we observed that the increased formation of LDs in control siRNA-treated cells exposed to PA and GW3965 was significantly reduced in *Scd1* K_D cells (Fig. 2C). To confirm that formation of LDs actively participated in cytoprotection from PA and were not passive bystanders, we knocked down *Dgat1* (diacylglycerol O-acyltransferase 1), which encodes a rate-limiting enzyme in LD formation. Our results proved that formation of LDs was critical to GW3965-mediated protection (Fig. S5A-C) because the action of *Dgat1* is downstream of SCD1 activity, and is not known to be directly regulated by NR1H/LXR. Taken together, these results showed that the NR1H/LXR agonist GW3965 protected against PA-induced lipotoxicity; moreover, this protection required GW3965 stimulation of *Scd1* expression and LD formation.

ULK1 is required for induction of *Scd1* expression and protection by GW3965 in PA-treated cells

Although the role of autophagy in lipotoxicity has been studied extensively,²³⁻²⁵ little is known about the effects of specific autophagic proteins on lipotoxicity. Moreover, the relative contributions and crosstalk between autophagy and autophagic proteins in counteracting lipotoxicity are not known. Using a public database, we found that gene expression of *Ulk1* was significantly downregulated in patients with NASH (Fig. S6), a condition that is associated with increased lipotoxicity in liver. Accordingly, we examined the cell autonomous effects of ULK1/ATG1 on lipotoxicity. In addition to inhibiting autophagy, we found that loss of ULK1 also significantly inhibited GW3965-mediated induction of SCD1 leading to increased lipotoxicity (as measured by CASP3 cleavage) in AML-12 cells (Fig. 3A, B). The effect of *Ulk1* K_D on GW3965-mediated induction of SCD1 expression was confirmed using 3 different *Ulk1* siRNAs (Fig. S7A). We further verified these results in primary mouse hepatocytes, which also exhibited impaired induction of *Scd1* mRNA by GW3965 when *Ulk1* was knocked down (Fig. S7B, C). To observe whether the effect on gene expression of *Ulk1* K_D was specific to *Scd1*, we analyzed the expression of several other NR1H/LXR target lipogenic genes such as *Fasn* and *Sreb1/Srebp1c*. qRT-PCR results revealed that loss of *Ulk1* significantly decreased the gene expression of *Scd1* and *Fasn* but had only a moderate effect on *Sreb1* (Fig. 3C-E). Additionally, microarray-based pathway analysis of cells treated with *Ulk1* siRNA vs. control siRNA did not show any impairment in the expression of genes involved in other classical NR1H/LXR-regulated targets such as ABC transporter (ATP-binding cassette transporter) genes (Table S1). These results strongly suggested that *Ulk1* K_D primarily affected the transcription of a selected lipogenic genes and did not cause a global

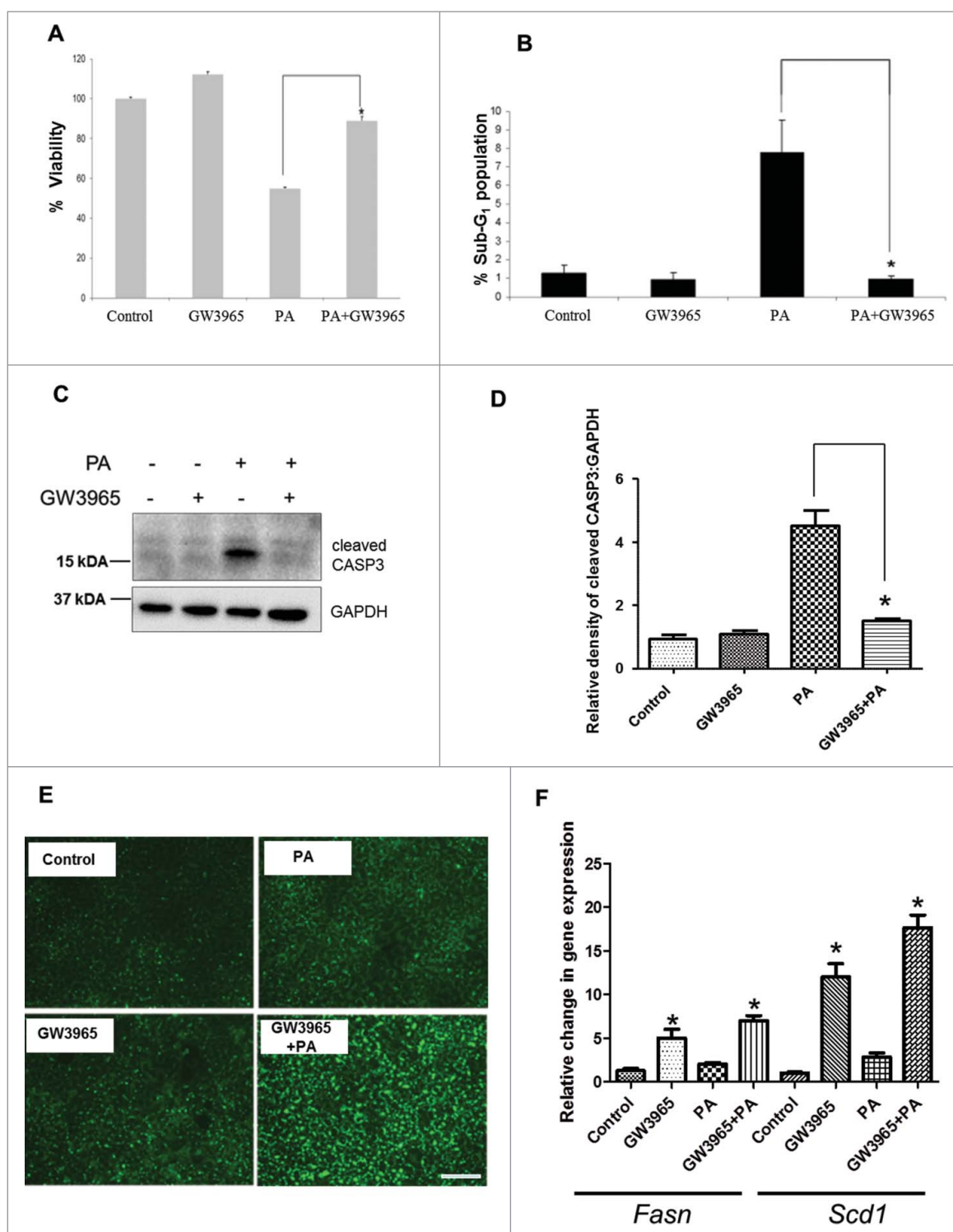


Figure 1. NR1H/LXR agonist GW3965 protects against PA-induced apoptosis. (A) MTS assay showing percent viability of AML-12 cells cotreated with 0.75 mM PA +/- 10 μ M GW3965 for 24 h. (B) Flow cytometric sub-G₁ peak analysis using propidium iodide staining of AML-12 cells cotreated with 0.75 mM PA +/- 10 μ M GW3965 for 24 h. (C, D) Representative immunoblot and densitometric analysis showing CASP3 cleavage products in AML-12 cells cotreated with 0.75 mM PA +/- 10 μ M GW3965 for 24 h. (E) Lipophilic fluorescent dye BODIPY 493/503 staining showing LDs (bright green stain) in AML-12 with 0.75 mM PA +/- 10 μ M GW3965 for 12 h (scale bar: 200 μ m). (F) qRT-PCR analysis showing *Scd1* and *Fasn* levels in AML-12 cells cotreated with 0.75 mM PA +/- 10 μ M GW3965 for 24 h. Bars represent the mean of the respective individual ratios \pm SD (n = 5, *p < 0.05).

impairment of NR1H/LXR-mediated transcriptional activity. In further support of this notion, we observed that the LD accumulation in hepatic cells treated with control siRNA and exposed to GW3965 and PA was reduced in *Ulk1* K_D cells (Fig. 3F). Collectively, these results confirmed that loss of *Ulk1* expression impaired the induction of *Scd1* mRNA

and formation of LDs by GW3965 in PA-treated cells, resulting in increased lipotoxicity. We also found similar effects of *Ulk1* K_D on SCD1 induction and protection from lipotoxicity by GW3965 in mouse C2C12 myoblast cells (data not shown) suggesting that ULK1 also had a similar role in protecting other cell types from lipotoxicity.

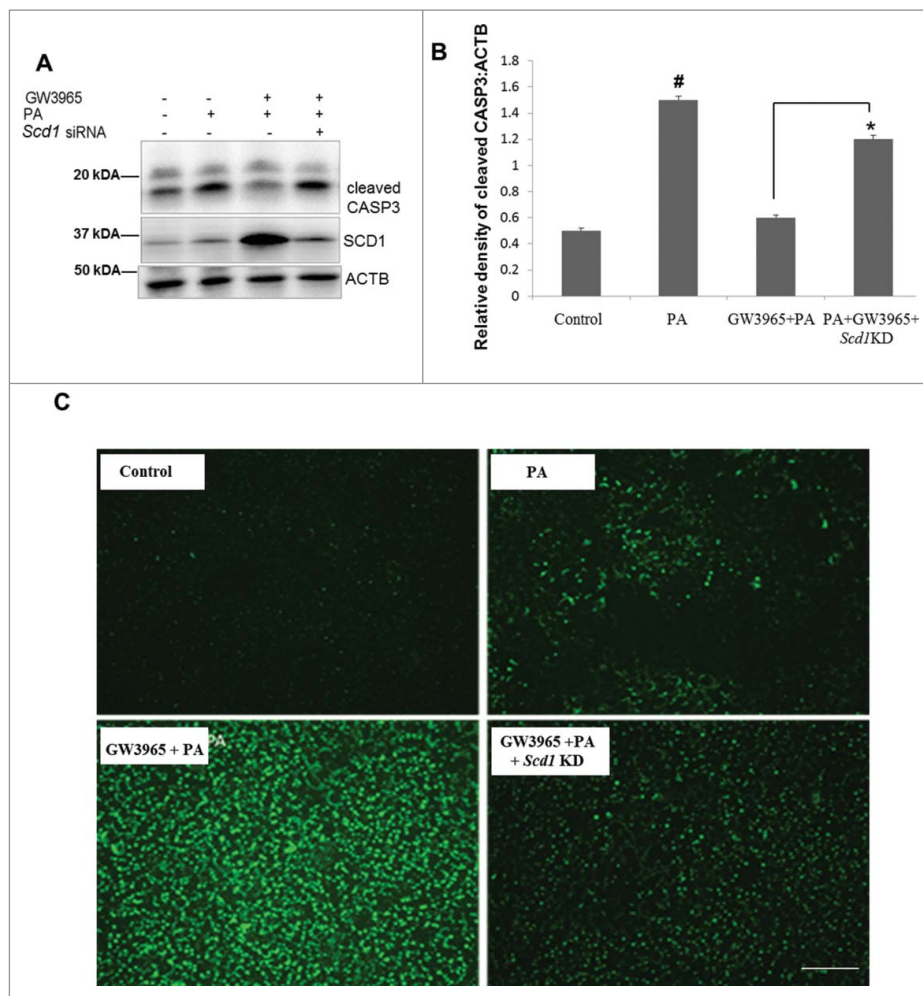


Figure 2. NR1H/LXR-induced *Scd1* is essential for GW3965-mediated protection against lipotoxicity. (A, B) Representative blots and densitometric analysis showing the effect of *Scd1* KD on apoptotic marker cleaved CASP3 (p17) and SCD1 in AML-12 cells cotreated with 0.75 mM PA +/- 10 μ M GW3965 for 24 h. Bars represent the mean of the respective individual ratios \pm SD (n = 5, #p < 0.05 denotes significant difference in cleaved CASP3 levels between PA vs. Control and PA + GW3965, *p < 0.05 denotes difference between PA + GW3965 + *Scd1* KD vs. PA + GW3965). (C) Lipophilic fluorescent dye BODIPY 493/503 staining showing LDs (bright green stain) in AML-12 cells +/- *Scd1* siRNA cotreated with 0.75 mM PA +/- 10 μ M GW3965 for 12 h (scale bar: 200 μ m).

ULK1 regulation of NR1H/LXR-mediated induction of *Scd1* expression requires its kinase domain but is independent of its autophagic function

ULK1 is a kinase that promotes autophagic activity by phosphorylating other ATG proteins. However, mutant ULK1 that lacked kinase activity has been also shown to exert other effects on cellular functions.⁴⁷ To determine whether the kinase activity of ULK1 was necessary for its effect on SCD1 expression, we used a recently described ULK1/2 inhibitor MRT0068921 to block its kinase activity.⁴⁸ This small molecule inhibitor previously was shown to interfere with the kinase activity of both ULK1 and ULK2 in vitro.⁴⁸ Our results demonstrated that the kinase domain of ULK1 was essential for SCD1 regulation since MRT0068921 significantly reduced the induction of SCD1 protein levels by GW3965 (Fig. 4A, B). *Ulk2* KD by siRNA also partially reduced the induction of SCD1 protein by GW3965 (Fig. S8). This reduced effect of *Ulk2* in comparison to *Ulk1* KD could be due to lower endogenous expression levels of *Ulk2* than *Ulk1* in AML-12 cells. Additionally, we observed that overexpression (OE) of wild-type (WT)

Ulk1 rescued the effect of *Ulk1* KD on GW3965-induced SCD1 protein levels and cell survival in hepatic cells, thus providing further evidence indicating that ULK1 kinase activity had a critical role in SCD1 expression (Fig. 4C-E).

Effects of ULK1 KD on GW3965-mediated *Scd1* expression are autophagy independent

We next asked whether the effects of ULK1 on *Scd1* expression and cytoprotection from PA were mediated by autophagy. Interestingly, the knockdown of other autophagic proteins such as RB1CC1/FIP200 (RB1-inducible coiled-coil 1) and BECN1 (Beclin 1, autophagy related) behaved similar to ULK1 knockdown, by decreasing GW3965-mediated protection from PA toxicity (Fig. 5A, B). In contrast, the effect on GW3965-mediated *Scd1* expression and LD formation only occurred with loss of *Ulk1* (Fig. 5C, D and Fig. S9A, B). These findings suggested that although the autophagic function of ULK1 and other autophagic proteins are needed for protection from PA-induced lipotoxicity, ULK1 regulation of *Scd1* and LD formation is an additional

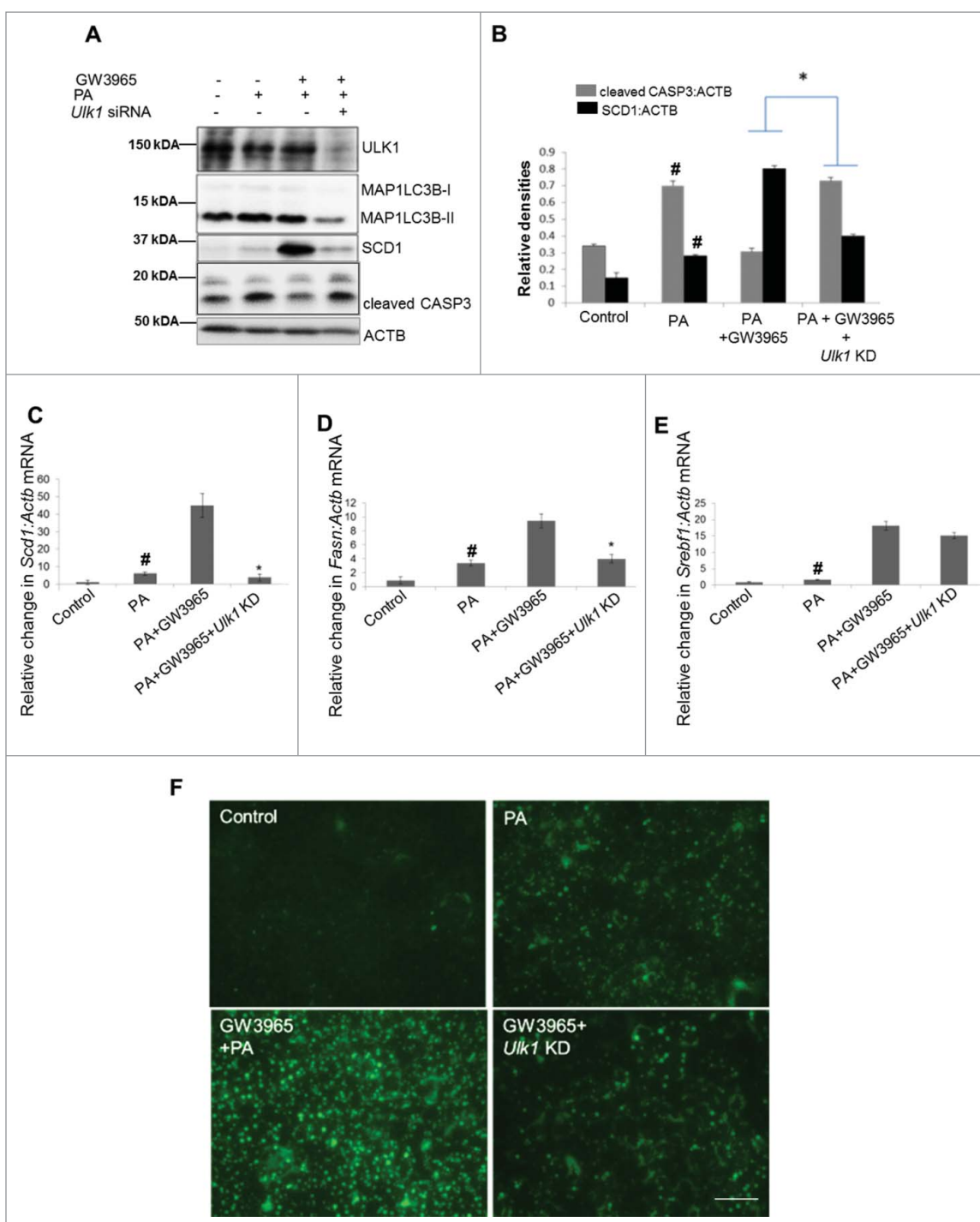


Figure 3. Loss of *Ulk1* impairs GW3965-induced SCD1 induction and protection from PA toxicity. (A, B) Representative blot and densitometric analysis showing the effect of *Ulk1* KD on apoptotic marker cleaved CASP3 (p17), autophagy marker MAP1LC3B-II and SCD1 in AML-12 cells cotreated with 0.75 mM PA +/- 10 μ M GW3965 for 24 h. Bars represent the mean of the respective individual ratios \pm SD (n = 5, [#]p < 0.05 denotes significant difference in cleaved CASP3 and SCD1 levels between PA vs. Control and PA + GW3965, ^{*}p < 0.05 denotes significant difference in cleaved CASP3 and SCD1 levels between PA + GW3965 vs. PA + GW3965 + *Ulk1* KD). (C-E) qRT-PCR analysis showing the effect of *Ulk1* KD on *Scd1*, *Fasn* and *Srebf1* levels in AML-12 cells cotreated with 0.75 mM PA +/- 10 μ M GW3965 for 24 h. (n = 5, [#]p < 0.05) (F) Lipophilic fluorescent dye BODIPY 493/503 staining showing LDs (bright green stain) in AML-12 cells +/- *Ulk1* siRNA cotreated with 0.75 mM PA +/- 10 μ M GW3965 for 12 h (scale bar: 200 μ m).

protective mechanism that is independent of autophagy. To demonstrate that ULK1s effect on expression of *Scd1* was critical to its role in the protection against lipotoxicity, we overexpressed *Scd1* in ULK1-knockdown cells, and could also partially rescue the deleterious effects of *Ulk1* KD on GW3965 induction of LD accumulation and lipotoxicity (Fig. 6A-C).

Loss of RPS6KB1 rescues NR1H/LXR-mediated induction of *Scd1* mRNA expression in ULK1-deficient cells

Because our results suggested ULK1 regulation of SCD1 was independent from autophagy, we examined signaling pathways known to be regulated by ULK1 activity. ULK1/Atg1 previously was shown to negatively regulate MTORC1-RPS6KB1 signaling

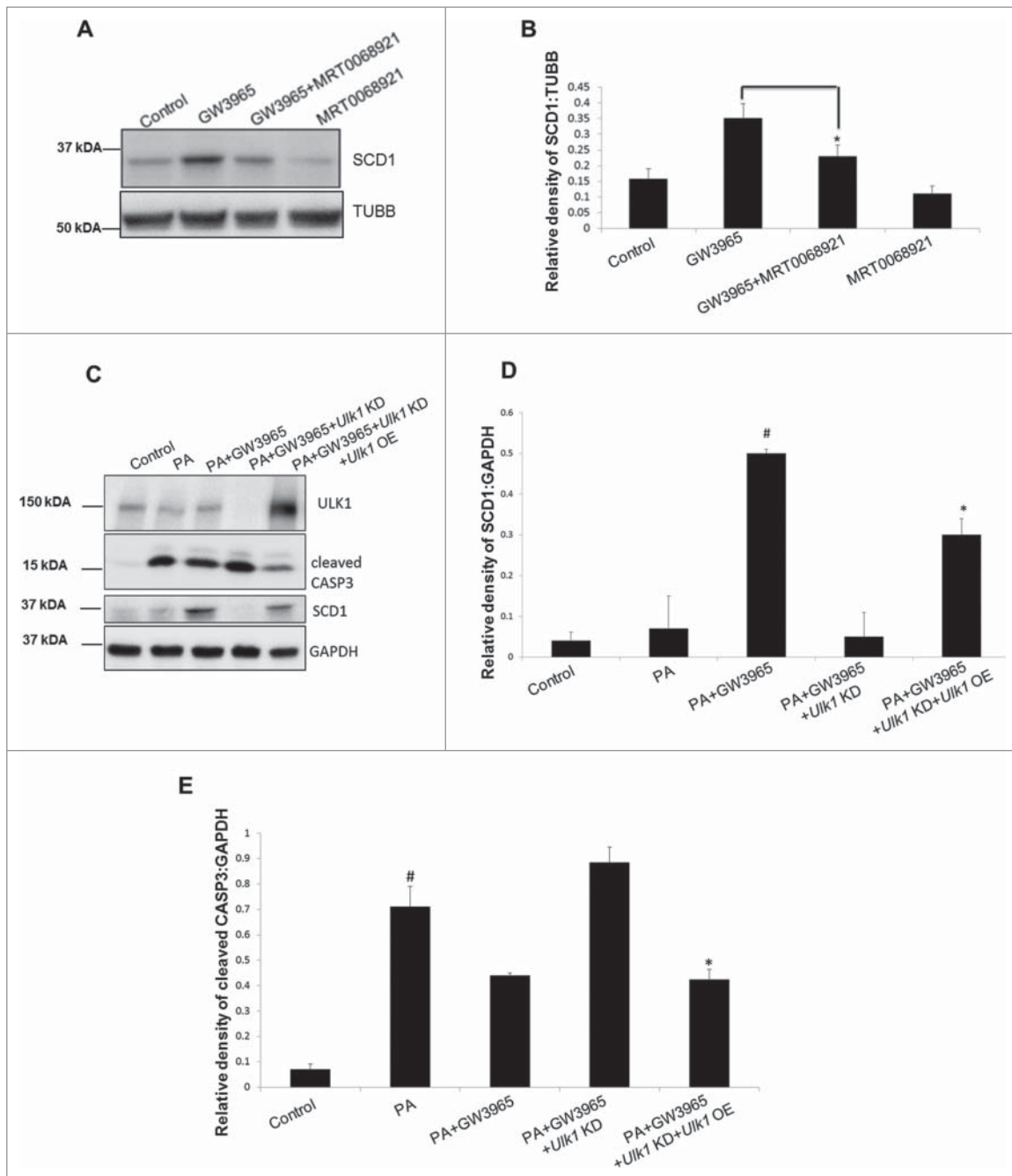


Figure 4. *Ulk1* kinase activity is required in regulating GW3965-mediated SCD1 expression. (A, B) Representative blot and densitometric analysis showing the effect of ULK1/2 kinase inhibitor MRT0068921 (1 μ M) on SCD1 levels in AML-12 cells treated with 10 μ M GW3965 for 24 h. Bars represent the mean of the respective individual ratios \pm SD (n = 5, *p < 0.05). (C-E) Representative blot and densitometric analysis showing the rescue effect of *Ulk1* overexpression (OE) in *Ulk1* K_D cells on SCD1 and CASP3 cleavage in AML-12 cells. Bars represent the mean of the respective individual ratios \pm SD (n = 5, #p < 0.05 denotes significant difference in cleaved CASP3 and SCD1 levels between PA vs. Control and PA + GW3965, *p < 0.05 denotes significant difference in cleaved CASP3 and SCD1 levels between PA + GW3965 + *Ulk1* K_D vs. PA + GW3965 + *Ulk1* K_D + *Ulk1* OE).

in yeast and mammalian cells.⁴⁹⁻⁵¹ We confirmed these findings in AML-12 cells by showing decreased phosphorylation of RPTOR and increased phosphorylation of RPS6KB1 in *Ulk1* K_D cells (Fig. 7A-D). Of note, the phosphorylation of another MTORC1 target, EIF4EBP1 also was increased in *Ulk1* K_D cells (data not shown).

RPS6KB1 activity has been previously associated with modulation of nuclear receptor signaling.^{52,53} Therefore, we next examined whether increased RPS6KB1 activity was involved in downregulating NR1H/LXR activity in these cells. Accordingly,

we knocked down *Rps6kb1* by siRNA in *Ulk1*-deficient cells and checked whether induction of SCD1 protein by GW3965 was affected. Indeed, knockdown of *Rps6kb1* rescued the induction of SCD1 expression in *Ulk1*-deficient cells treated with GW3965 (Fig. 7E, F). Furthermore, concomitant with the increase in SCD1, *Rps6kb1* K_D also restored the cytoprotective effect of GW3965 against PA-induced lipotoxicity in *Ulk1* K_D cells as evidenced by decreased cleaved CASP3 (Fig. 7E, F) and formation of lipid droplets (Fig. S10). However, to our surprise, specific pharmacological inhibition of RPS6KB1 activity, but

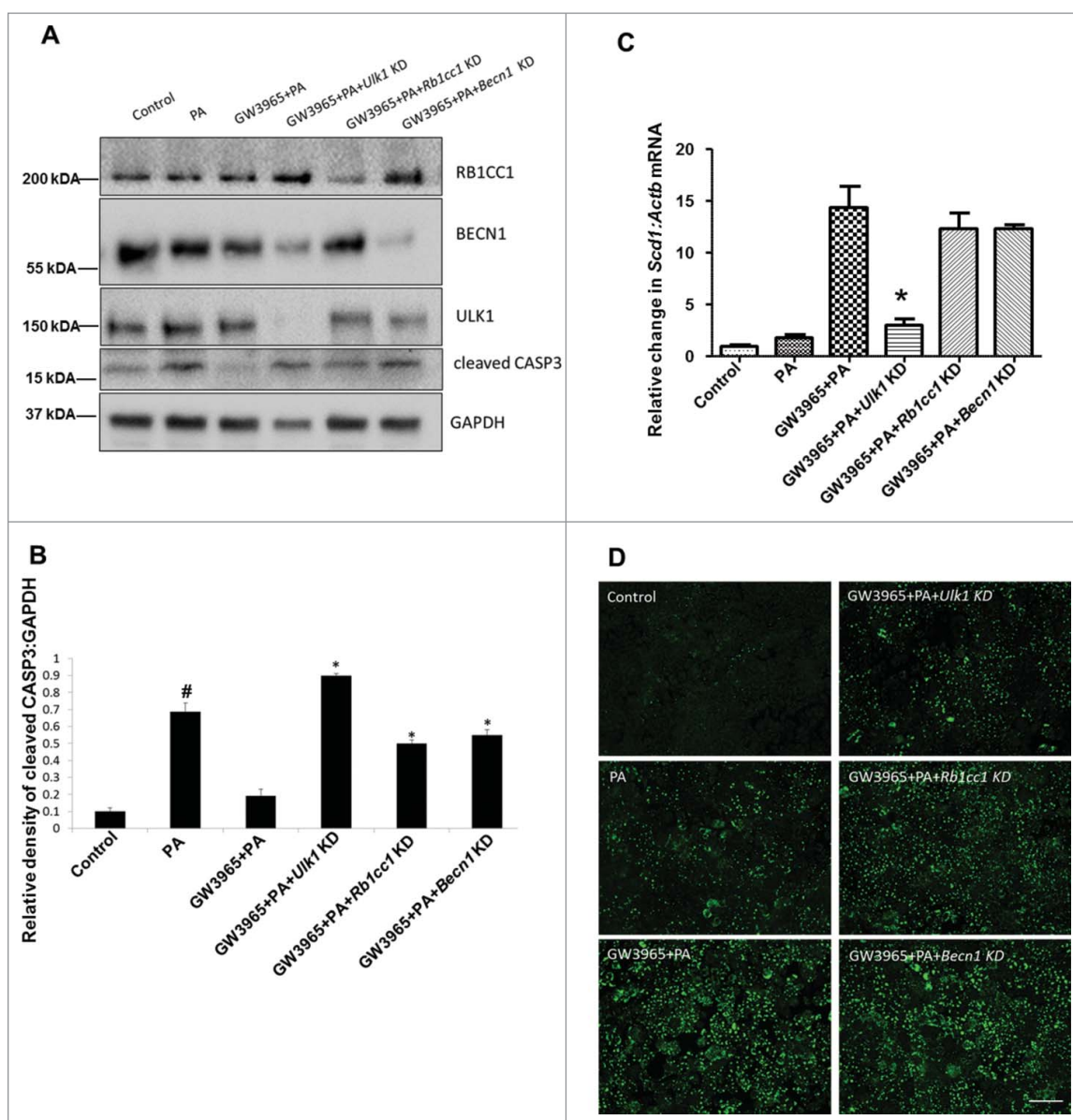


Figure 5. ULK1 regulation of NR1H/LXR-mediated SCD1 expression is independent of autophagy. (A, B) Representative blot and densitometric analysis showing comparative effect of *Ulk1*, *Rb1cc1* and *Becn1* K_D treatment on CASP3 cleavage levels in AML-12 cells treated with 0.75 mM PA +/- 10 μ M GW3965 for 24 h (n = 5, [#]p < 0.05 denotes significant difference in cleaved CASP3 levels between PA vs. Control and PA + GW3965, *p < 0.05 denotes significant difference in cleaved CASP3 levels between PA + GW3965 vs. PA + GW3965 + *Ulk1*, *Rb1cc1* or *Becn1* K_D). (C) qRT-PCR analysis showing comparative effect of *Ulk1*, *Rb1cc1* and *Becn1* K_D treatment on *Scd1* mRNA levels in AML-12 cells treated with 0.75 mM PA +/- 10 μ M GW3965 for 24 h (n = 5, *p < 0.05 denotes significant difference between PA + GW3965 vs. PA + GW3965 + *Ulk1*, *Rb1cc1* or *Becn1* K_D). (D) BODIPY 493/503 staining showing comparative effect of *Ulk1*, *Rb1cc1* and *Becn1* K_D treatment on LD formation in AML-12 cells treated with 0.75 mM PA +/- 10 μ M GW3965 for 12 h (scale bar: 200 μ m).

not inhibition of pan-MTOR activity, rescued the effect of *Ulk1* K_D on GW3965-induced SCD1 expression (Fig. S11). Taken together, our findings showed that increased RPS6KB1 activity played a major role in the inhibition of NR1H/LXR-mediated induction of *Scd1* transcription and the increased apoptosis caused by loss of *Ulk1* expression in a lipotoxic condition.

RPS6KB1 stimulates NCOR1 nuclear localization and interaction with NR1H/LXR in *Ulk1*-deficient cells

MTORC1-RPS6KB1 signaling previously was shown to inhibit PPARA/PPAR α (peroxisome proliferator activated receptor α) transcriptional activity by increasing its interaction with the nuclear corepressor NCOR1.^{52,53} Besides its ability to repress

PPARA-mediated transcription, NCOR1 also is a potent repressor of NR1H/LXR-mediated transcription.^{20,54,55} Since RPS6KB1 was activated when *Ulk1* was knocked down, we examined whether a similar repression of NR1H/LXR target genes by NCOR1 could occur in *Ulk1* K_D cells. Indeed, we observed that NCOR1 nuclear localization was increased in *Ulk1* K_D cells compared to control cells based upon immunoblotting of nuclear fractions and immunofluorescence of NCOR1 in *Ulk1* K_D cells (Fig. 8A, B). Strikingly, this effect of *Ulk1* K_D on NCOR1 nuclear recruitment was lost when *Rps6kb1* was knocked down (Fig. 8A-C). These results were consistent with earlier reports showing the direct involvement of *Rps6kb1/2* in increasing NCOR1 nuclear translocation.^{52,53}

We then performed coimmunoprecipitation experiments to examine intracellular NCOR1 and NR1H/LXR interaction.

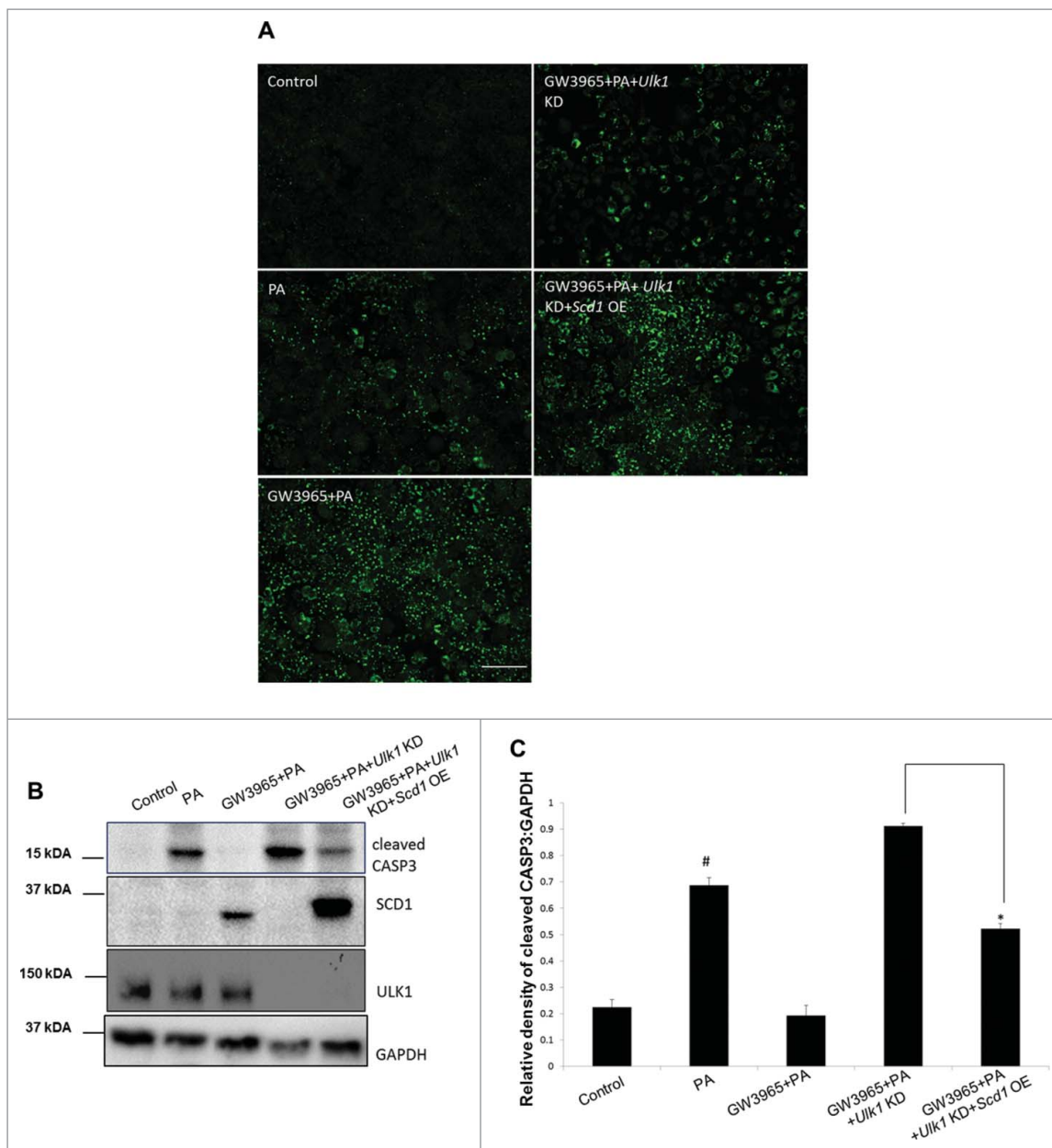


Figure 6. Ectopic expression of SCD1 rescues the effect of *Ulk1* K_D on GW3965-induced LD formation and cell survival. (A) BODIPY 493/503 staining showing comparative effect of *Scd1* overexpression (OE) treatment on LD formation in AML-12 cells treated with 0.75 mM PA +/- 10 μM GW3965 for 12 h in a background of *Ulk1* K_D (scale bar: 200 μm). (C, D) Representative blot and densitometric analysis showing the rescue effect of *Scd1* overexpression (OE) in *Ulk1* K_D cells on CASP3 cleavage in AML-12 cells. Bars represent the mean of the respective individual ratios ±SD (n = 5, [#]p < 0.05 denotes significant difference in cleaved CASP3 levels between PA vs. Control and PA + GW3965, ^{*}p < 0.05 denotes significant difference in cleaved CASP3 levels between PA + GW3965 + *Ulk1* K_D vs. PA + GW3965 + *Ulk1* K_D + *Scd1* OE.

Interestingly, our results showed increased interaction between NR1H3/LXRα and NCOR1 in *Ulk1* K_D cells (Fig 9A,B). These results were further strengthened by ChIP-qPCR analysis showing increased recruitment of NCOR1 to the region spanning the NR1H/LXRE within the *Scd1* gene promoter in *Ulk1* K_D cells (Fig. 9C). These findings suggested that increased NR1H3/LXRα–NCOR1 interaction could lead to repression of *Scd1* transcription.

***Ncor1* K_D rescues inhibition of NR1H/LXR-mediated induction of *Scd1* and lipotoxicity in *Ulk1*-deficient hepatic cells**

Because NCOR1 is a common repressor of several nuclear receptors, we wanted to confirm whether its interaction with NR1H/

LXRs mediates its effects on *Scd1* transcription. To do so, we transfected either WT *Ncor1* or NR1H/LXR-TR binding-deficient mutant (Δ ID) *Ncor1*²⁰ into GW3965-treated cells and observed their effect on *Scd1* expression. The results showed that overexpression of WT *Ncor1* inhibited GW3965 induction of *Scd1* whereas Δ ID had no effect (Fig. 10A). Consistent with this finding, *Ncor1* K_D partially prevented the downregulation of *Scd1* expression in *Ulk1* K_D cells treated with GW3965 (Fig. 10B–D) at both mRNA and protein levels. Similarly, *Ncor1* K_D also significantly rescued the effect of *Ulk1* K_D on *Scd1* and CASP3 cleavage in a lipotoxic environment (Fig. 10E, F).

Taken together, our results suggested that in *Ulk1* K_D cells, RPS6KB1 becomes activated and leads to increased

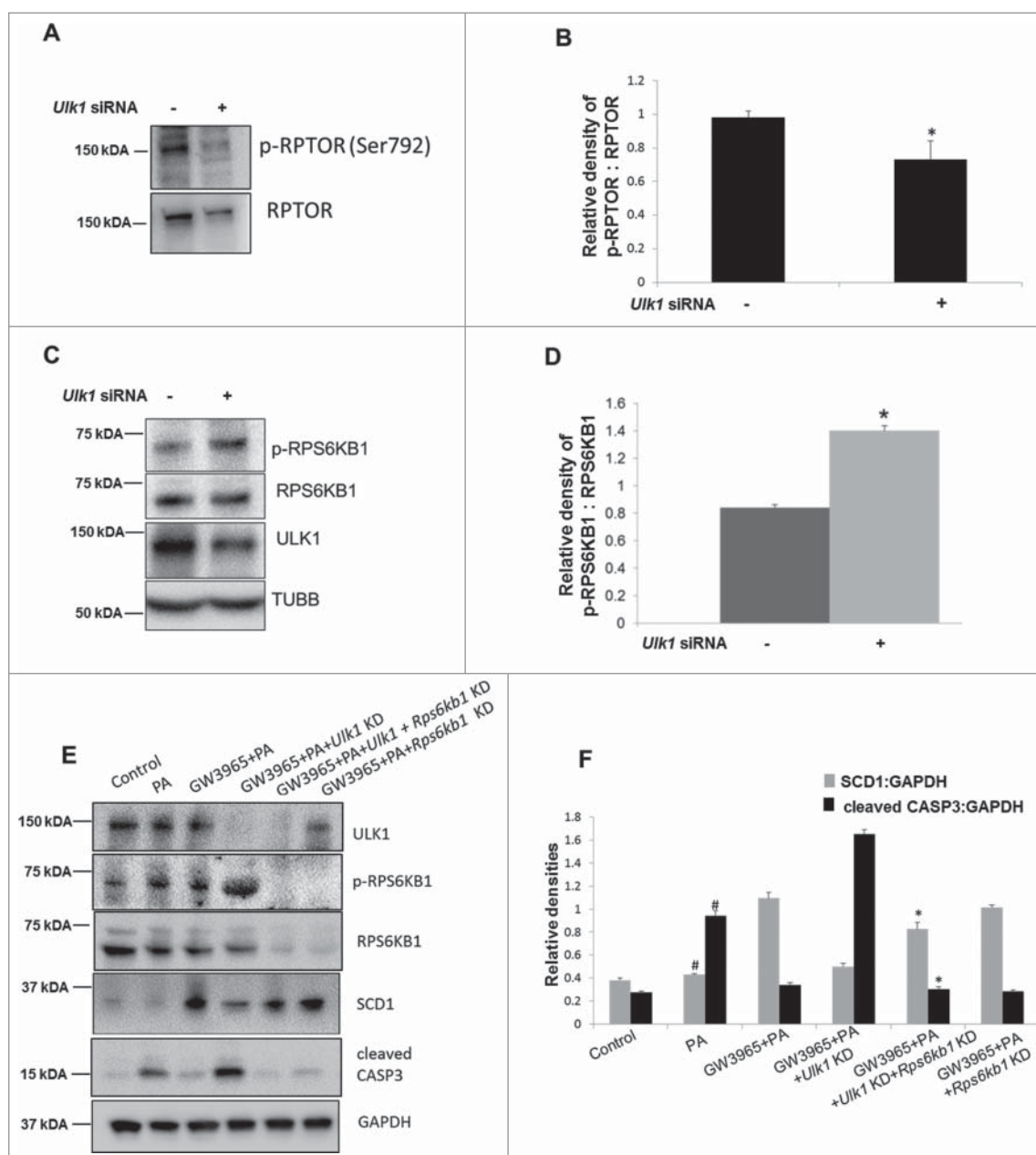


Figure 7. Upregulated RPS6KB1 activity mediates suppression of SCD1 in *Ulk1* K_D cells. (A, B) Representative blot and densitometric analysis showing p-RPTOR:RPTOR levels in AML-12 after 48 h of *Ulk1* K_D. Bars represent the mean of the respective individual ratios \pm SD (n = 5, *p < 0.05). (C, D) Representative blot and densitometric analysis showing p-RPS6KB1:RPS6KB1 levels in AML-12 after 48 h of *Ulk1* K_D. Bars represent the mean of the respective individual ratios \pm SD (n = 5, *p < 0.05). (E, F) Representative blot and densitometric analysis showing the effect of *Ulk1* K_D +/- RPS6KB1 K_D on SCD1 and cleaved CASP3 levels in AML-12 cells cotreated with 0.75 mM PA +/- 10 μ M GW3965 for 24 h. Bars represent the mean of the respective individual ratios \pm SD (n = 5, #p < 0.05 denotes significant difference in cleaved CASP3 and SCD1 levels between PA vs. Control and PA + GW3965, *p < 0.05 denotes significant difference in cleaved CASP3 and SCD1 levels between PA + GW3965 + *Ulk1* K_D vs. PA + GW3965 + *Ulk1* K_D + *Rps6kb1* K_D).

nuclear uptake of NCOR1 (Fig. 11). This, in turn, increases NCOR1 interaction with NR1H/LXRs and its co-recruitment to the NR1HE on the *Scd1* promoter to repress NR1H/LXR-mediated transcription of this gene. Decreased *Scd1* gene expression then leads to decreased intracellular conversion of SFAs to MUFAs resulting in less lipid droplet formation and increased intracellular accumulation of SFAs and increased lipotoxicity. Thus, this process opposes the cytoprotective effect of NR1H/LXR ligand on PA-induced lipotoxicity.

Discussion

The rapid rise in the incidence of lipid-associated metabolic diseases such as obesity, diabetes and NASH has generated strong interest in the pathogenesis and treatment of "lipotoxicity."⁶ SFAs released from adipose tissue can generate toxic metabolites in peripheral organs such as liver and muscle, and induce mitochondrial dysfunction, caspase activation, and apoptosis.⁶ In contrast, cells exposed to unsaturated fatty acids accumulate triglycerides in LDs and channel saturated fatty acids into less toxic

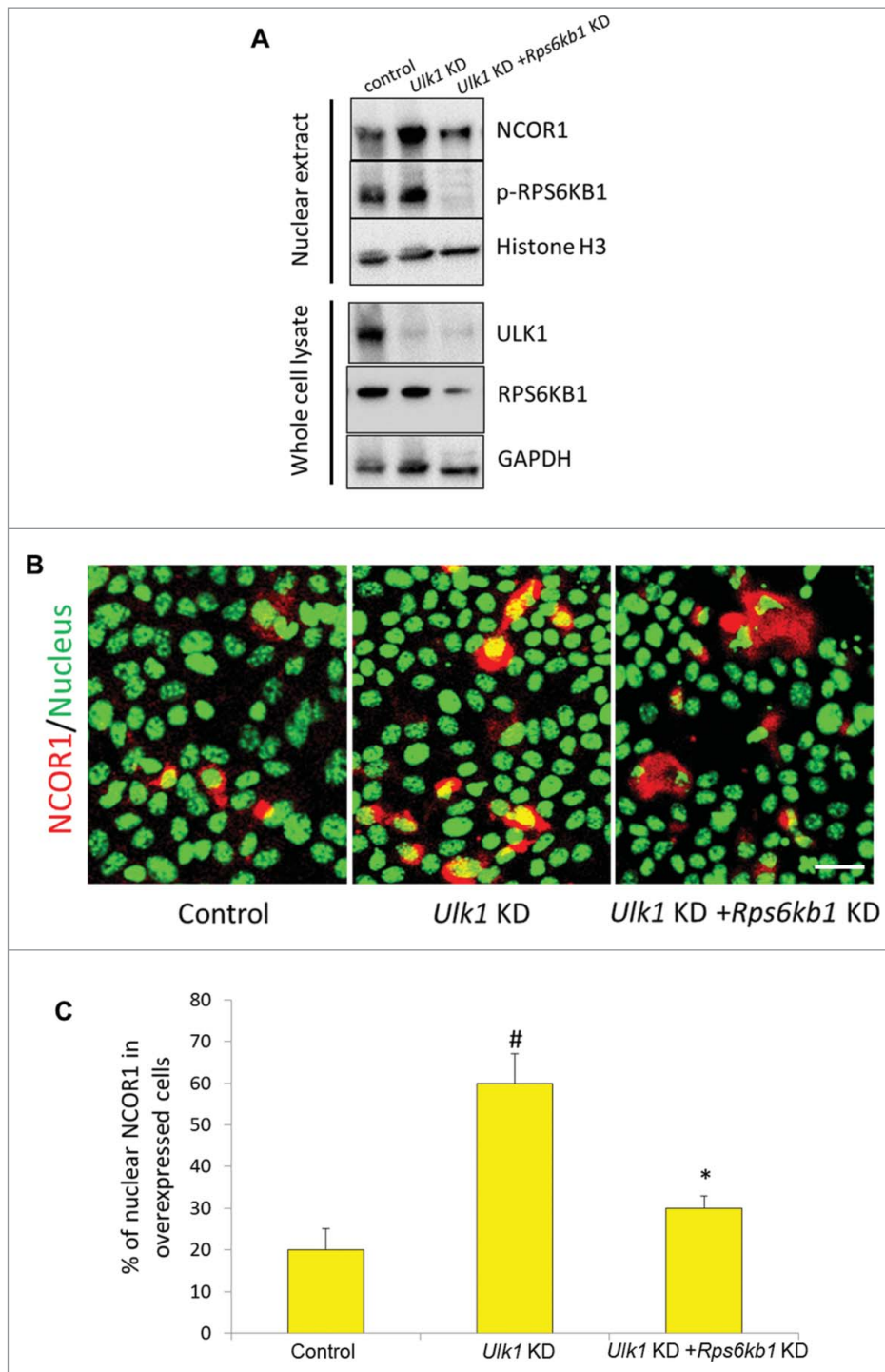


Figure 8. RPS6KB1 drives NCOR1 nuclear localization upon loss of ULK1 activity. (A) Representative immunoblot shows the level of NCOR1 in nuclear extracts in control, *Ulk1* KD and *Ulk1* + *Rps6kb1* double knockdown AML-12 cells. Whole cell lysates were used to assess the knockdown efficiency. (B, C) Representative immunofluorescence image and quantification of NCOR1-FLAG-transfected cells using anti-FLAG antibody (red) and DAPI (green pseudo color) in cells treated with *Ulk1* alone or *Ulk1* + *RPS6KB1* siRNA for 48 h (scale bar: 200 μ m). Bars represent the mean of the respective individual ratios \pm SD (n = 5, [#]p < 0.05 denotes significant between *Ulk1* KD vs. *Ulk1* KD + *Rps6kb1* KD cells. Control and, ^{*}p < 0.05 denotes significant difference between *Ulk1* KD vs. *Ulk1* KD + *Rps6kb1* KD cells.

lipid pools that reduce oxidative stress.^{9,56,57} Genes such as *Scd1* are pivotal for converting saturated fatty acids to less toxic unsaturated ones that can be stored in LDs.¹⁵ Ligand-bound NR1H/LXRs can directly stimulate *Scd1* transcription,⁴⁶ and reduce lipotoxicity by converting SFAs into MUFAs and inducing LD formation. Indeed, NR1H/LXR agonists increase triglyceride packaging into LDs by stimulating *Scd1* gene expression¹⁶ and

thus decrease lipotoxicity by reducing intracellular SFA concentration and their conversion into toxic metabolites that cause oxidative damage, ER stress, and apoptosis.

In addition to LD formation, the cell employs autophagy as an important mechanism to protect itself from lipotoxicity.⁵⁸ Downregulation of autophagic flux and autophagic protein levels have been closely associated with increased lipotoxicity in

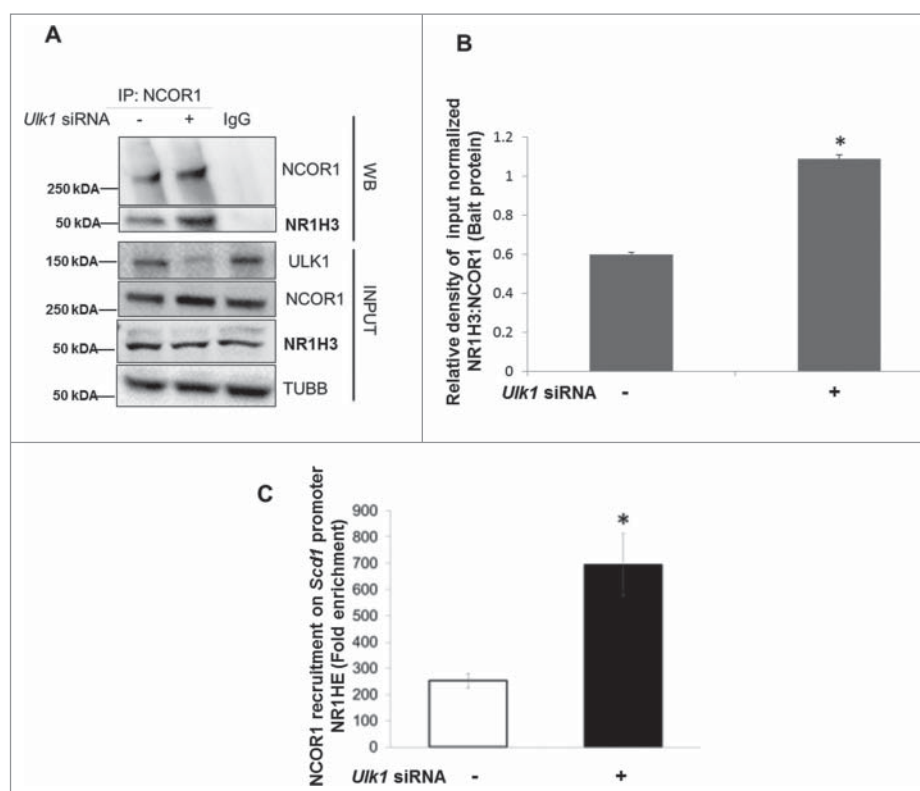


Figure 9. *Ulk1* K_D increases NCOR1-NR1H3/LXR interaction and NCOR1 recruitment to *Scd1* promoter NR1HEs. (A, B) Representative blot and densitometric analysis following Co-IP of NR1H3/LXR α using NCOR1 antibody in cells treated +/- *Ulk1* siRNA for 48 h. For quantifying the NR1H3/LXR α -NCOR1 interaction as shown in panel (B), relative densities of affinity isolated NR1H3/LXR α and NCOR1 were first normalized to their levels in the Input and later in the IP samples +/- *Ulk1* K_D . (C) ChIP-qPCR analysis of NCOR1 recruitment to NR1HE on the *Scd1* promoter in cells treated +/- *Ulk1* siRNA for 48 h. Bars represent the mean of the respective individual ratios \pm SD (n = 3, *p < 0.05).

metabolic diseases.⁵⁸⁻⁶⁵ However, the specific role(s) of autophagy genes in protecting cells from lipotoxicity is not well understood. Furthermore, it is possible that autophagy proteins may have autophagy-independent functions that may help reduce lipotoxicity. In this study, we investigated the role of the autophagy protein ULK1 in decreasing lipotoxicity induced by SFAs in hepatic cells. Our findings showed that loss of either ULK1 expression or activity increased apoptosis when cells were exposed to lipotoxic concentrations of PA. *Ulk1* deficiency decreased cell survival and was associated with decreased LD formation and *Scd1* expression under these conditions. Our results showed that although autophagy is needed to protect against lipotoxicity, the effect of *Ulk1* K_D on *Scd1* mRNA and protein expression, as well as LD formation is specific and not shared by other autophagy proteins that we examined. Although the autophagic arm of *Ulk1* and other autophagy genes seems to provide cytoprotection from PA, an autophagy-independent arm of *Ulk1* regulates *Scd1* expression, and provides further cytoprotection from lipotoxicity.

It is noteworthy that LD and autophagosome formation frequently are spatially and temporally associated with each other.⁶⁶ Both of these organelles originate from the ER membrane and appear to be mutually dependent since common gene networks regulate their formation and the impairment of either of them often affects the function or expression of the other.^{33,67-69} Thus, our results are consistent with earlier findings that demonstrated the role of autophagy genes in the formation of LDs in *C. elegans* and mammalian cells.^{32,33} Here, we showed that the formation

of LDs specifically required ULK1 activity but was independent of the autophagic function of ULK1. Similarly, in this connection, another autophagy protein, MAP1LC3/Atg8 was shown to be recruited to the nascent LD surface and participate in LD formation.³⁵ Thus, autophagy proteins may have other important nonautophagic cellular functions.⁷⁰ Indeed, ULK1 recently was shown to participate in several other nonautophagic signaling pathways associated with cell growth and survival.⁴²⁻⁴⁴ Similar to our findings, ULK1/Atg1 negatively regulates RPS6KB1 signaling either directly or indirectly by inhibiting MTORC1 activity.⁴⁹⁻⁵¹ It is also noteworthy to point here that inhibition of TORC1 activity in yeast increases LD accumulation,⁷¹ suggesting the possibility of an evolutionarily conserved common mechanism for LD formation via modulation of ULK1 and MTORC1 activity. Although our results suggest that ULK1 employs a nonautophagic mechanism of cytoprotection, nevertheless we cannot exclude the possibility that increased SCD1 levels and LDs themselves may also contribute to an autophagic role of ULK1 to reduce lipotoxicity. This issue becomes even more relevant since LDs themselves now have been recognized as having a major role in autophagosome formation.^{69,72,73}

Our results showed that loss of *Ulk1* led to activation of RPS6KB1 signaling and repression of *Scd1* gene expression. It is known that MTORC1-RPS6KB1 signaling often is upregulated in obesity and associated metabolic diseases.⁶¹ Since MTORC1 and ULK1 mutually inhibit each other, it is possible that an increase in MTORC1-RPS6KB1 signaling could aggravate lipotoxic injury in tissues by decreasing both *Scd1* gene expression

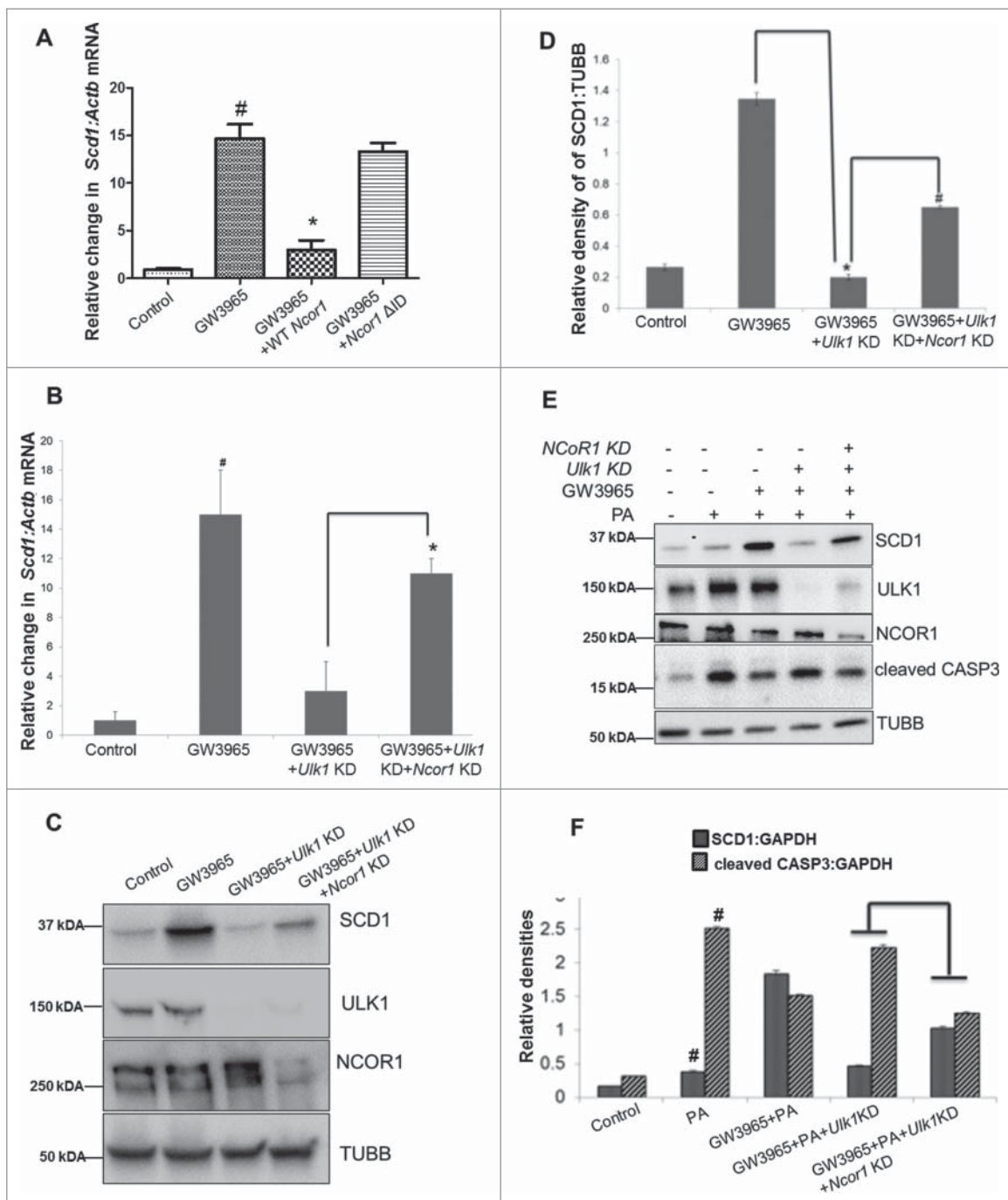


Figure 10. NCOR1-mediated inhibition of NR1H/LXR-induced SCD1 expression increases lipotoxicity in hepatic cells. (A) qRT-PCR analysis showing the effect of WT and Δ ID mutant NCOR1 overexpression on GW3965 (10 μ M/24 h)-induced SCD1 expression in AML-12 cells. Bars represent the mean of the respective individual ratios \pm SD ($n = 3$, # $p < 0.05$ denotes significant difference between Control and GW3965, * $p < 0.05$ denotes significant difference between GW3965 vs. GW3965 + WT *Ncor1* overexpression). (B) qRT-PCR analysis showing the effect of *Ulk1* K_D +/- *Ncor1* K_D on *Scd1* mRNA levels in AML-12 cells treated with 10 μ M GW3965 for 24 h. Bars represent the mean of the respective individual ratios \pm SD ($n = 5$, # $p < 0.05$ denotes significant difference in *Scd1* mRNA levels between GW3965 vs. Control and GW3965 + *Ulk1* K_D , * $p < 0.05$ denotes significant difference in *Scd1* mRNA levels between GW3965 + *Ulk1* K_D vs. GW3965 + *Ulk1* K_D + *Ncor1* K_D). (C, D) Representative blot and densitometric analysis showing the effect of *Ulk1* K_D +/- *Ncor1* K_D on SCD1 levels in AML-12 cells treated with 10 μ M GW3965 for 24 h. Bars represent the mean of the respective individual ratios \pm SD ($n = 5$, # $p < 0.05$). (E, F) Representative blot and densitometric analysis showing the effect of *Ulk1* K_D +/- *Ncor1* K_D on SCD1 and cleaved CASP3 levels in AML-12 cells cotreated with 0.75 mM PA +/- 10 μ M GW3965 for 24 h. Bars represent the mean of the respective individual ratios \pm SD ($n = 5$, # $p < 0.05$ denotes significant difference in cleaved CASP3 and SCD1 levels between PA vs. Control and PA + GW3965, * $p < 0.05$ denotes significant difference between cleaved CASP3 and SCD1 levels between PA + GW3965 + *Ulk1* K_D vs. PA + GW3965 + *Ulk1* K_D + *Ncor1* K_D).

and autophagy in these conditions. In this connection, a pro-lipotoxic role of RPS6KB1 has been observed in human hepatocytes.⁷⁴ Our results indicate that although loss of ULK1 increases MTORC1 activity with the concomitant activation of RPS6KB1, the regulation of SCD1 by ULK1 seems to be exclusively RPS6KB1-mediated. The reason for this paradoxical

finding is that although both knockdown (Fig. 7E,F) and pharmacological inhibition (Fig. S10) of RPS6KB1 reverses the effect of *Ulk1* K_D on *Scd1* expression, the same effect was not observed with pan-MTOR inhibitors such as Torin1 (Fig. S10) or rapamycin (data not shown). These results could be due to an RPS6KB1-independent, and possibly antagonistic, regulation of *Scd1*, via a

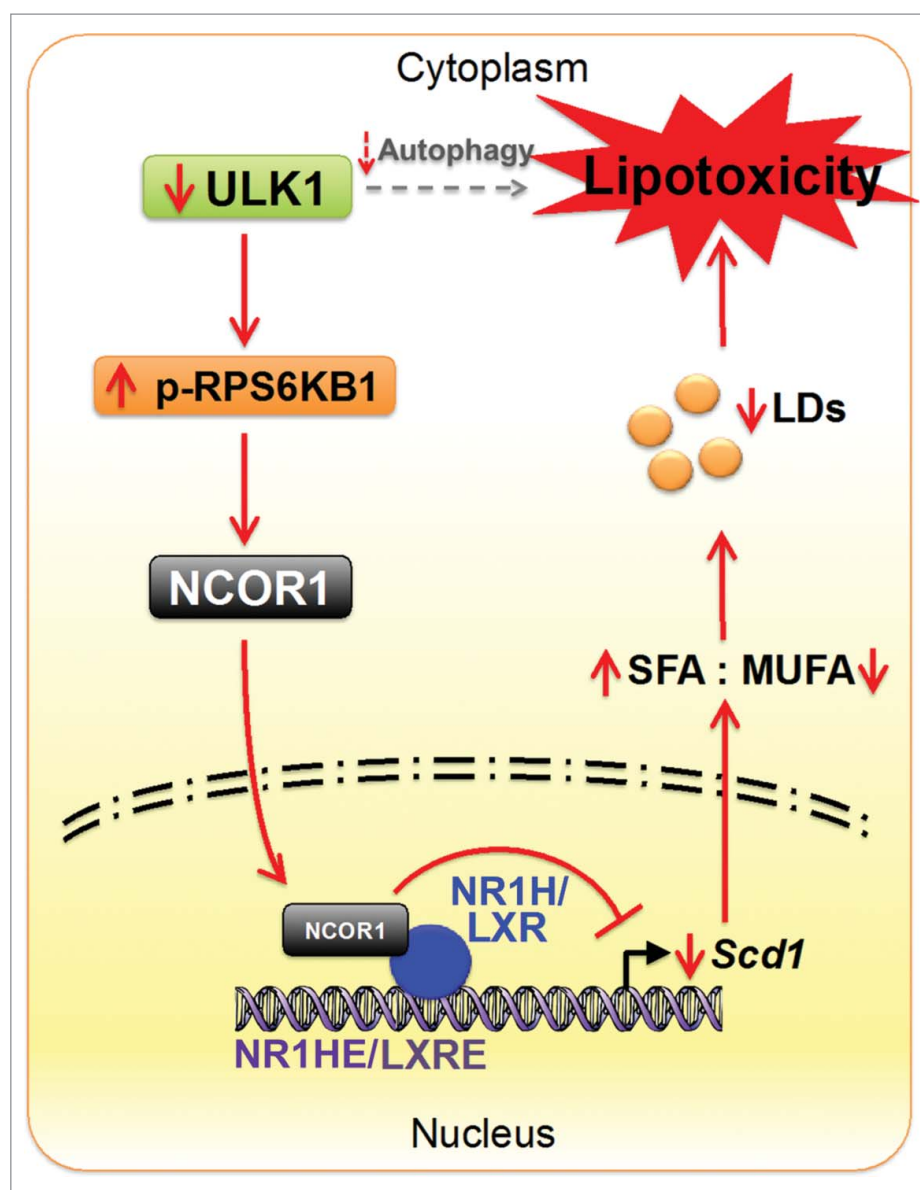


Figure 11. Proposed model elucidating the effect of ULK1 loss on SFA-induced lipotoxicity in cells. Our study suggests that besides the impairment of autophagy-mediated signaling, ULK1 downregulation in a lipotoxic environment leads to increased activation of RPS6KB1. This in turn causes increased nuclear localization of NCOR1 in the nucleus. NCOR1-mediated inactivation of NR1H/LXRs causes suppression of *Scd1* transcription hence leading to an increased SFA/MUFA ratio. This would further decrease the generation of neutral LDs and eventually cause cell death via lipotoxicity.

separate MTORC1 signaling pathway. Such an effect has been previously shown for the regulation of SREBF1 which is MTOR dependent but RPS6KB1 independent in rat hepatocytes.⁷⁵ Thus, it is possible that inhibiting general MTOR activity by Torin1 or rapamycin may decrease other pro-lipogenic signaling effects, and cancel out any increase in *Scd1* expression brought upon by the loss of RPS6KB1 activity. These possibilities notwithstanding, our findings strongly show that RPS6KB1 mediates ULK1-dependent regulation of SCD1 by GW3965.

Recent studies have shown that MTORC1-RPS6KB1 can alter nuclear receptor signaling by increasing the phosphorylation and nuclear localization of the nuclear corepressor NCOR1.^{52,53} NCOR1 is a transcriptional coregulatory protein that contains several nuclear receptor interacting domains. Upon binding to nuclear receptor complexes that are associated with nuclear receptor response elements within the DNA promoter regions of target genes, NCOR1 recruits histone deacetylases that induce

histone decetylation to repress transcription.⁷⁶ In this connection, livers from mice lacking functional NCOR1 had increased expression of several NR1H/LXR target genes including *Scd1*.²⁰ When taken together with our results, it is likely that a RPS6KB1-driven increase in NCOR1-NR1H/LXR interaction accounts for the inhibition of *Scd1* transcription observed in *Ulk1* K_D cells. However, it is important to note that *Ncor1* K_D did not rescue *Scd1* expression to the same extent as RPS6KB1 K_D in *Ulk1*-deficient cells treated with GW3965. This finding suggests that RPS6KB1-mediated suppression of *Scd1* gene expression may involve other pathways besides NCOR1 phosphorylation and nuclear localization. Another intriguing observation was the selectivity of NR1H/LXR target genes affected by *Ulk1* K_D. Our results showed that GW3965-induced transcription was impaired for several lipogenic genes whereas other NR1H/LXR target genes such as the ABC transporter protein involved in reverse cholesterol transport⁷⁷ were not affected.

The reason for this selective effect of *Ulk1* K_D is not known; however, it is possible that differential co-repressor recruitment⁷⁸ or a corepressor-independent effect of *Ulk1* K_D on other NR1H/LXR target genes may be involved.

In summary, we have identified a novel autophagy-independent function of ULK1 in hepatic cells that involves inhibition of RPS6KB1 signaling and NCOR1-mediated repression of NR1H/LXR-regulated *Scd1* gene expression. Decreased *Ulk1* expression leads to repression of *Scd1* expression, decreased LD formation, and increased lipotoxicity and apoptosis. Our study thus demonstrates that ULK1 plays an important role in preventing lipotoxicity in mammalian hepatic cells by regulating *Scd1* gene expression. Although the roles of upstream regulators such as AMPK and MTORC1 on ULK1 phosphorylation and autophagy have been well characterized,⁷⁹ little was known previously about an autophagy-independent role for ULK1 in metabolic diseases. Interestingly, we have observed a significant downregulation of *Ulk1* in livers from patients with NASH that was not observed in patients with benign hepatosteatosis using a public microarray database⁶⁴ (Fig S6). These results suggest that decreased *Ulk1* expression may contribute to the hepatic lipotoxicity in NASH.

Since SCD1 has a pivotal role in preventing lipotoxicity by desaturating SFAs and facilitating LD formation, restoration of *Ulk1* expression and/or activity may potentially enhance the protective action of NR1H/LXRs in NASH and other metabolic conditions. Accordingly, enhancement of ULK1 expression/activity or inhibition of RPS6KB1 activity may be a novel strategy for the treatment of lipotoxicity-induced diseases such as NASH when there already are manifestations of hepatic lipotoxicity. Previously, there have been concerns about the use of NR1H/LXR agonists in NAFLD since they promote lipogenesis and hepatosteatosis. Our findings suggest that these notions for NR1H/LXR agonists may need to be reconsidered in the context of NASH, particularly when lipotoxicity becomes a significant feature of NAFLD as ULK1-mediated regulation of *Scd1* transcription and LD formation may offer protection to hepatic cells when challenged under such conditions.

Materials and methods

Reagents

Antibody details are as follows: LC3B (Cell Signaling Technology, 2775), ULK1 (Cell Signaling Technology, 8054), RPS6KB1/p70 S6 kinase (Cell Signaling Technology, 2708), phospho-RPS6KB1/p70 S6 kinase (Thr389; Cell Signaling Technology, 9234), GAPDH (Cell Signaling Technology, 5174), TUBB/ β -tubulin (Cell Signaling Technology, 2146), BECN1/Beclin 1 (Cell Signaling Technology, 3738), cleaved CASP3/caspase3 (Cell Signaling Technology, 9664), RB1CC1/FIP200 (Cell Signaling Technology, 12436), FASN/fatty acid synthase (Cell Signaling Technology, 3180), ACTB/ β -Actin (Santa Cruz Biotechnology, sc-81178), SCD1 (Santa Cruz Biotechnology, sc-14720), and ULK2 (Santa Cruz Biotechnology, sc-10907). Culture media and transfection reagents were from Invitrogen, USA. siRNA used are as follows: *Ulk1* (Ambion[®], s75751), *Ulk2* (Ambion[®], s78109), *Rb1cc1* (Ambion[®], s63494), *Scd1* (Ambion[®], s73339), *Becn1* (Ambion[®], s80166), *Atg5* (Ambion[®], s62453), *Rpskb1*

(Ambion[®], s91055), *Ncor1* (Ambion[®], s73228), *Dgat1* (Ambion[®], s64953), *Fasn* (Ambion[®], s65867), *Cpt1a* (Ambion[®], s64347) and *Ulk1* (Dharmacon, LU-040155-00-0002). MRT0068921 was a kind gift from Dr. Barbara Saxty (MRC, UK). pcdna3 flag - *Ulk1* WT was a gift from Reuben Shaw (Addgene plasmid, 27636).⁴¹ NCOR1 antibody used for immunoblotting has been described earlier.²⁰ Other chemicals were GW3965 (SIGMA-ALDRICH, G6295), palmitic acid (SIGMA-ALDRICH, P0500), oleic acid (SIGMA-ALDRICH, O1008), Torin1 (Tocris Bioscience, 4247), PF4708671 (Tocris Bioscience, 4032), PBS (SIGMA-ALDRICH, P3813) and SCD1 inhibitor (ABCAM, ab142089).

Cell culture

AML-12 (CRL-2254) cells were maintained at 37°C in DMEM-F12 1:1 containing 10% fetal bovine serum, 1x ITS (ThermoFisher Scientific, 41400), 10 nM dexamethasone and 1x penicillin/streptomycin in a 5% CO₂ atmosphere. For siRNA transfection, cells were transfected using RNAiMAX (Thermo Fisher Scientific, 13778) with either specific siRNAs or negative siRNAs, and for overexpression experiments, Lipofectamine 3000 (Thermo Fisher Scientific, L3000001) with gene specific or empty plasmids, following the manufacturer's reverse-transfection protocol. Primary mouse hepatocytes were isolated and cultured using a standard 2-step collagenase perfusion protocol.⁸⁰ For knockdown studies, cells were treated with specific siRNA (10 nM) for 24-48 h before adding PA and GW3965. PA was prepared in the culture medium containing 2% BSA (SIGMA-ALDRICH, A4612) and added to cells for 12 or 24 h as indicated. The control cells were cultured in medium containing 2% BSA. Cells were cotreated with GW3965 and other drugs along with PA wherever mentioned.

RNA isolation and real-time PCR

Total RNA was isolated and qPCR performed using the QuantiTect SYBR Green PCR Kit (Qiagen, 204141) in accordance with the manufacturer's instructions. Primer sequence were *Scd1*: 5'-GTGGGGTAATTATTTGTGACC-3' (sense) 5'-TTTTTCCCAGACAGTACAAC-3' (antisense), *Fasn*: 5'-CGGATTCGGTGTATCCTGCT-3' (sense) 5'-CCTCGGGTGAGGACGT TTAC-3' (antisense), *Srebf1*: 5'-ATCGGCGCGGAAGCTGTCGGGGTAGCGTC-3' (sense) 5'-ACTGTCTTGGTTGTTGATGAGCTGGAGCAT-3' (antisense), *Actb* 5'-GATGTATGAA GGCTTTGGTC-3' (sense) 5'-TGTGCACTTTTATTGGTCTC-3' (antisense).

MicroArray and KEGG pathway analysis

Gene expression microarray profiling was performed using the MouseWG-6 v2.0 Expression BeadChip Kit (Illumina, BD-201-0202). cRNA generation, labeling and hybridization were performed at Duke-NUS Genome Biology Facility, Duke-NUS Graduate Medical School, Singapore. Gene expression signals were quantile normalized, and differentially expressed genes were identified via analysis of variance, using treatment-specific contrasts (Partek Genomics Suite software, version 6.6). Statistical significance of differentially expressed genes was

ascertained in terms of the false discovery rate. Complete dataset was submitted to GEO repository (GSE74059). Principal components analysis (PCA) based on gene expression demonstrated a clear separation between the 3 experimental groups and no outliers. Pathway enrichment analysis was conducted via the Gene Set Enrichment Analysis tool using a list of KEGG pathways extracted from the Molecular Signatures Database. For analysis of *Ulk1* expression in human NASH and steatosis a publically available database was used.⁶⁴ The data set is accessible at the ArrayExpress public repository for microarray data under the accession number E-MEXP-3291 (<http://www.webcitation.org/5zyojNu7T>). The distribution of *Ulk1* gene expression in Control, NASH and steatotic samples was ascertained via boxplots, and the statistical significance of expression differences across the 3 groups was determined via ANOVA. All calculations were performed in the statistical package, R 3.2.3.

Western blotting

Cells or tissue samples were lysed using CelLytic™ M Cell Lysis Reagent (Sigma, C2978) and immunoblotting was performed as described previously.⁴⁰ Image acquisition was done using ChemiDoc (Bio-Rad ChemiDoc™ MP System, 1708280). Densitometry analysis was performed using ImageJ software (NIH, Bethesda, MD, USA).

Immunofluorescence studies

Immunofluorescence experiments were performed as described previously.⁴⁰ In brief formalin-fixed cells were permeabilized with 0.1% Triton X-100 (SIGMA-ALDRICH, X100) in PBS for 5-10 min and blocked with 3% BSA-PBS for 30 min at room temperature. Cells were incubated with the primary antibody (1:200 in 3% BSA-PBS) overnight at 4°C and cell imaging was performed using an Operetta® High Content Imaging System (PerkinElmer, MA, USA). BODIPY 493/503 (Thermo Fisher Scientific, D3922) was dissolved in ethanol to give a stock of 1 mg/ml. Cells were stained for 15 min at 1:1000 dilution, washed with PBS 3 times, and observed using an Olympus fluorescence microscope and 20X magnification. TUNEL assay was performed as per the manufacturer's instructions using the In Situ Cell Death Detection Kit, Fluorescein (Roche, 11684795910).

Lipid peroxidation measurement

Lipid peroxidation was measured using the TBARS Assay Kit (CAYMAN CHEMICALS, 10009055).

Transmission electron microscopy

Cells were seeded onto 4-chambered coverglass (Lab-tek Chambered Coverglass System, Nalgene-Nunc, Rochester, NY, USA) at a density of 2×10^4 cells/ml (14,000 cells/well). After treatment cells were fixed with 2.5% glutaraldehyde and washed 3 times with PBS. Subsequent post-fixation with 1% osmium tetroxide followed by dehydration with an ascending series of alcohol before embedding samples in araldite (SIGMA-ALDRICH, A3183). Ultrathin sections were cut and doubly stained with

uranyl acetate and lead citrate. Images were acquired using the Olympus EM208S transmission electron microscope.

Viability and apoptosis measurements

Cell viability was assessed using CellTiter 96® Aqueous One Solution Cell Proliferation (MTS) Assay (Promega, G3582). For the sub-G₁ peak assay to measure apoptosis cells were harvested and fixed in 70% (vol/vol) ethanol. The cells were then stained with propidium iodide for 20 min in the dark. At least 1×10^5 stained cells were analyzed for sub-G₁ profile on a (MACSQuant Analyzer 10, Miltenyi Biotec, Germany). The results presented are averages and standard deviations from 3 separate experiments.

NCOR1 IP and ChIP

Immunoprecipitation was performed with antibodies against control IgG and NCOR1 antibodies using the immunoprecipitation starter pack (GE Healthcare, 17-6002-35) as per the manufacturer's protocol followed by immunoblotting. The ChIP assays was performed using EZ-Magna ChIP™ G-Chromatin Immunoprecipitation Kit (Millipore, 17-610) according to the provided protocol.

Eluted DNA was purified with the QIAamp DNA Mini Kit (Qiagen, 51304). Immune-precipitated DNA (2 μl) and 1% input DNA was used with QuantiFast SYBR Green PCR Kit (QIAGEN) for 40 cycles of qPCR using the Rotor-Gene® Q qPCR machine (Qiagen). A primer set spanning the *Scd1* promoter NR1HEs from -1140 to -1033 (forward primer 5' GCTCCACCATACACTGGCTA 3' and reverse primer 5' GTCTGCCTTTGAGCTGGGTC 3') was used to analyze NCOR1 binding to the NR1HE/LXR response element (NR1HE: TGACCAcaggTAACCT)

Calculations and statistics

Results were expressed as mean ± SD. The statistical significance of differences (**P* < 0.05) was assessed by ANOVA analyses followed by Tukey's post-hoc when comparing different groups.

Abbreviations

ACTB	actin β
BECN1	Beclin 1, autophagy related
CASP3	caspase 3
FASN	fatty acid synthase
K _D	knockdown
LXRs	liver X receptors
LDs	lipid droplets
MAP1LC3	microtubule-associated protein 1 light chain 3
MTOR	mechanistic target of rapamycin (serine/threonine kinase)
MUFAs	mono-unsaturated fatty acids
NASH	nonalcoholic steatohepatitis
NCOR1	nuclear receptor co-repressor 1
NR1HE	NR1H response element

OA	oleic acid
PA	palmitic acid
PRKAA1	protein kinase
AMP-activated	α 1 catalytic subunit
RPS6KB1/p70S6K1	ribosomal protein S6 kinase, polypeptide 1
SCD1	stearoyl-CoenzymeA desaturase 1
SFAs	saturated fatty acids
SQSTM1/p62	sequestosome 1
TUBB	tubulin, β
ULK1	unc-51 like kinase 1

Disclosure of potential conflicts of interest

No potential conflicts of interest were disclosed.

Acknowledgments

We would like to thank Andrea Lim, and Yu Guang, (Duke-NUS, Singapore) as well as Drs. Barbara Saxty (MRC, UK), Inna Astapova (Beth Israel Deaconess Medical Center and Harvard Medical School, Boston, USA), and Kristmundur Sigmundsson (Duke-NUS, Singapore), Yajun Wu (NUS, Singapore) and Prof. Bay Boon-Huat (NUS, Singapore) for their helpful advice, technical support, and valuable reagents.

Funding

This work was supported by NMRC/CSA/ 0054/2013 (PMY), NMRC/CIRG/1340/2012 (PMY), and from Singapore Ministry of Health NMRC/BNIG/2025/2014 (RAS). We are thankful to Dr. Vinay Tergaonkar (IMCB, Singapore) our collaborator and Co-PI in the NMRC/BNIG/2025/2014 grant for his support.

References

- [1] Tumova J, Andel M, Trnka J. Excess of free fatty acids as a cause of metabolic dysfunction in skeletal muscle. *Physiol Res* 2015; PMID:26447514
- [2] Brenner C, Galluzzi L, Kepp O, Kroemer G. Decoding cell death signals in liver inflammation. *J Hepatol* 2013; 59:583-94; PMID:23567086; <http://dx.doi.org/10.1016/j.jhep.2013.03.033>
- [3] Cusi K. The role of adipose tissue and lipotoxicity in the pathogenesis of type 2 diabetes. *Curr Diab Rep* 2010; 10:306-15; PMID:20556549; <http://dx.doi.org/10.1007/s11892-010-0122-6>
- [4] Ibrahim SH, Kohli R, Gores GJ. Mechanisms of lipotoxicity in NAFLD and clinical implications. *J Pediatr Gastroenterol Nutr* 2011; 53:131-40; PMID:21629127; <http://dx.doi.org/10.1097/MPG.0b013e31820e82a1>
- [5] Neuschwander-Tetri BA. Hepatic lipotoxicity and the pathogenesis of nonalcoholic steatohepatitis: the central role of nontriglyceride fatty acid metabolites. *Hepatology* 2010; 52:774-88; PMID:20683968; <http://dx.doi.org/10.1002/hep.23719>
- [6] Rial E, Rodriguez-Sanchez L, Gallardo-Vara E, Zaragoza P, Moyano E, Gonzalez-Barroso MM. Lipotoxicity, fatty acid uncoupling and mitochondrial carrier function. *Biochim Biophys Acta* 2010; 1797:800-6; PMID:20388489; <http://dx.doi.org/10.1016/j.bbabi.2010.04.001>
- [7] Savary S, Trompier D, Andreoletti P, Le Borgne F, Demarquoy J, Lizard G. Fatty acids - induced lipotoxicity and inflammation. *Curr Drug Metab* 2012; 13:1358-70; PMID:22978392; <http://dx.doi.org/10.2174/138920012803762729>
- [8] Cazanave SC, Gores GJ. Mechanisms and clinical implications of hepatocyte lipoapoptosis. *Clin Lipidol* 2010; 5:71-85; PMID:20368747; <http://dx.doi.org/10.2217/clp.09.85>
- [9] Listenberger LL, Han X, Lewis SE, Cases S, Farese RV, Jr., Ory DS, Schaffer JE. Triglyceride accumulation protects against fatty acid-induced lipotoxicity. *Proc Natl Acad Sci U S A* 2003; 100:3077-82; PMID:12629214; <http://dx.doi.org/10.1073/pnas.0630588100>
- [10] Asai T, Okumura K, Takahashi R, Matsui H, Numaguchi Y, Murakami H, Murakami R, Murohara T. Combined therapy with PPAR α agonist and L-carnitine rescues lipotoxic cardiomyopathy due to systemic carnitine deficiency. *Cardiovasc Res* 2006; 70:566-77; PMID:16546150; <http://dx.doi.org/10.1016/j.cardiores.2006.02.005>
- [11] McClain CJ, Barve S, Deaciuc I. Good fat/bad fat. *Hepatology* 2007; 45:1343-6; PMID:17538963; <http://dx.doi.org/10.1002/hep.21788>
- [12] Chaurasia B, Summers SA. Ceramides - Lipotoxic Inducers of Metabolic Disorders. *Trends Endocrinol Metab* 2015; 26:538-50; PMID:26412155; <http://dx.doi.org/10.1016/j.tem.2015.07.006>
- [13] Flowers MT, Ntambi JM. Role of stearoyl-coenzyme A desaturase in regulating lipid metabolism. *Curr Opin Lipidol* 2008; 19:248-56; PMID:18460915; <http://dx.doi.org/10.1097/MOL.0b013e3282f9b54d>
- [14] Stamatikos AD, Paton CM. Role of stearoyl-CoA desaturase-1 in skeletal muscle function and metabolism. *Am J Physiol Endocrinol Metab* 2013; 305:E767-75; PMID:23941875; <http://dx.doi.org/10.1152/ajpendo.00268.2013>
- [15] Li ZZ, Berk M, McIntyre TM, Feldstein AE. Hepatic lipid partitioning and liver damage in nonalcoholic fatty liver disease: role of stearoyl-CoA desaturase. *J Biol Chem* 2009; 284:5637-44; PMID:19119140; <http://dx.doi.org/10.1074/jbc.M807616200>
- [16] Peter A, Weigert C, Staiger H, Rittig K, Cegan A, Lutz P, Machicao F, Häring HU, Schleicher E. Induction of stearoyl-CoA desaturase protects human arterial endothelial cells against lipotoxicity. *Am J Physiol Endocrinol Metab* 2008; 295:E339-49; PMID:18523127; <http://dx.doi.org/10.1152/ajpendo.00022.2008>
- [17] Peter A, Weigert C, Staiger H, Machicao F, Schick F, Machann J, Stefan N, Thamer C, Häring HU, Schleicher E. Individual stearoyl-coa desaturase 1 expression modulates endoplasmic reticulum stress and inflammation in human myotubes and is associated with skeletal muscle lipid storage and insulin sensitivity in vivo. *Diabetes* 2009; 58:1757-65; PMID:19478146; <http://dx.doi.org/10.2337/db09-0188>
- [18] Masuda M, Miyazaki-Anzai S, Keenan AL, Okamura K, Kendrick J, Chonchol M, Offermanns S, Ntambi JM, Kuro-O M, Miyazaki M. Saturated phosphatidic acids mediate saturated fatty acid-induced vascular calcification and lipotoxicity. *J Clin Invest* 2015; 125:4544-58; PMID:26517697
- [19] Matsui H, Yokoyama T, Sekiguchi K, Iijima D, Sunaga H, Maniwa M, Ueno M, Iso T, Arai M, Kurabayashi M. Stearoyl-CoA desaturase-1 (SCD1) augments saturated fatty acid-induced lipid accumulation and inhibits apoptosis in cardiac myocytes. *PLoS One* 2012; 7:e33283; PMID:22413010
- [20] Astapova I, Lee LJ, Morales C, Tauber S, Bilban M, Hollenberg AN. The nuclear corepressor, NCoR, regulates thyroid hormone action in vivo. *Proc Natl Acad Sci U S A* 2008; 105:19544-9; PMID:19052228; <http://dx.doi.org/10.1073/pnas.0804604105>
- [21] Chu K, Miyazaki M, Man WC, Ntambi JM. Stearoyl-coenzyme A desaturase 1 deficiency protects against hypertriglyceridemia and increases plasma high-density lipoprotein cholesterol induced by liver X receptor activation. *Mol Cell Biol* 2006; 26:6786-98; PMID:16943421; <http://dx.doi.org/10.1128/MCB.00077-06>
- [22] Feng Y, Yao Z, Klionsky DJ. How to control self-digestion: transcriptional, post-transcriptional, and post-translational regulation of autophagy. *Trends Cell Biol* 2015; 25:354-63; PMID:25759175; <http://dx.doi.org/10.1016/j.tcb.2015.02.002>
- [23] Mei S, Ni HM, Manley S, Bockus A, Kassel KM, Luyendyk JP, Copple BL, Ding WX. Differential roles of unsaturated and saturated fatty acids on autophagy and apoptosis in hepatocytes. *J Pharmacol Exp Ther* 2011; 339:487-98; PMID:21856859; <http://dx.doi.org/10.1124/jpet.111.184341>
- [24] Tan SH, Shui G, Zhou J, Li JJ, Bay BH, Wenk MR, Shen HM. Induction of autophagy by palmitic acid via protein kinase C-mediated signaling pathway independent of mTOR (mammalian target of rapamycin). *J Biol Chem* 2012; 287:14364-76; PMID:22408252; <http://dx.doi.org/10.1074/jbc.M111.294157>
- [25] Mir SU, George NM, Zahoor L, Harms R, Guinn Z, Sarvetnick NE. Inhibition of autophagic turnover in β -cells by fatty acids and glucose leads to apoptotic cell death. *J Biol Chem* 2015; 290:6071-85; PMID:25548282; <http://dx.doi.org/10.1074/jbc.M114.605345>

- [26] Khan MJ, Rizwan Alam M, Waldeck-Weiermair M, Karsten F, Groschner L, Riederer M, Hallström S, Rockenfeller P, Konya V, Heinemann A, et al. Inhibition of autophagy rescues palmitic acid-induced necroptosis of endothelial cells. *J Biol Chem* 2012; 287:21110-20; PMID:22556413; <http://dx.doi.org/10.1074/jbc.M111.319129>
- [27] Li S, Du L, Zhang L, Hu Y, Xia W, Wu J, Zhu J, Chen L, Zhu F, Li C, et al. Cathepsin B contributes to autophagy-related 7 (Atg7)-induced nod-like receptor 3 (NLRP3)-dependent proinflammatory response and aggravates lipotoxicity in rat insulinoma cell line. *J Biol Chem* 2013; 288:30094-104; PMID:23986436; <http://dx.doi.org/10.1074/jbc.M113.494286>
- [28] Liu K, Czaja MJ. Regulation of lipid stores and metabolism by lipophagy. *Cell Death Differ* 2013; 20:3-11; PMID:22595754; <http://dx.doi.org/10.1038/cdd.2012.63>
- [29] Singh R, Kaushik S, Wang Y, Xiang Y, Novak I, Komatsu M, Tanaka K, Cuervo AM, Czaja MJ. Autophagy regulates lipid metabolism. *Nature* 2009; 458:1131-5; PMID:19339967; <http://dx.doi.org/10.1038/nature07976>
- [30] Sinha RA, Farah BL, Singh BK, Siddique MM, Li Y, Wu Y, Ilkayeva OR, Gooding J, Ching J, Zhou J, et al. Caffeine stimulates hepatic lipid metabolism by the autophagy-lysosomal pathway in mice. *Hepatology* 2014; 59:1366-80; PMID:23929677; <http://dx.doi.org/10.1002/hep.26667>
- [31] Sinha RA, You SH, Zhou J, Siddique MM, Bay BH, Zhu X, Privratsky ML, Cheng SY, Stevens RD, Summers SA, et al. Thyroid hormone stimulates hepatic lipid catabolism via activation of autophagy. *J Clin Invest* 2012; 122:2428-38; PMID:22684107; <http://dx.doi.org/10.1172/JCI60580>
- [32] Rambold AS, Cohen S, Lippincott-Schwartz J. Fatty acid trafficking in starved cells: regulation by lipid droplet lipolysis, autophagy, and mitochondrial fusion dynamics. *Dev Cell* 2015; 32:678-92; PMID:25752962; <http://dx.doi.org/10.1016/j.devcel.2015.01.029>
- [33] Lapierre LR, Silvestrini MJ, Nunez L, Ames K, Wong S, Le TT, Hansen M, Meléndez A. Autophagy genes are required for normal lipid levels in *C. elegans*. *Autophagy* 2013; 9:278-86; PMID:23321914; <http://dx.doi.org/10.4161/auto.22930>
- [34] Ma D, Molusky MM, Song J, Hu CR, Fang F, Rui C, Mathew AV, Pennathur S, Liu F, Cheng JX, et al. Autophagy deficiency by hepatic FIP200 deletion uncouples steatosis from liver injury in NAFLD. *Mol Endocrinol* 2013; 27:1643-54; PMID:23960084; <http://dx.doi.org/10.1210/me.2013-1153>
- [35] Shibata M, Yoshimura K, Furuya N, Koike M, Ueno T, Komatsu M, Arai H, Tanaka K, Kominami E, Uchiyama Y. The MAP1-LC3 conjugation system is involved in lipid droplet formation. *Biochem Biophys Res Commun* 2009; 382:419-23; PMID:19285958; <http://dx.doi.org/10.1016/j.bbrc.2009.03.039>
- [36] Chan EY, Kir S, Tooze SA. siRNA screening of the kinome identifies ULK1 as a multidomain modulator of autophagy. *J Biol Chem* 2007; 282:25464-74; PMID:17595159; <http://dx.doi.org/10.1074/jbc.M703663200>
- [37] Ganley IG, Lam du H, Wang J, Ding X, Chen S, Jiang X. ULK1, ATG13, FIP200 complex mediates mTOR signaling and is essential for autophagy. *J Biol Chem* 2009; 284:12297-305; PMID:19258318; <http://dx.doi.org/10.1074/jbc.M900573200>
- [38] Hosokawa N, Hara T, Kaizuka T, Kishi C, Takamura A, Miura Y, Iemura S, Natsume T, Takehana K, Yamada N, et al. Nutrient-dependent mTORC1 association with the ULK1-Atg13-FIP200 complex required for autophagy. *Mol Biol Cell* 2009; 20:1981-91; PMID:19211835; <http://dx.doi.org/10.1091/mbc.E08-12-1248>
- [39] Wong PM, Puente C, Ganley IG, Jiang X. The ULK1 complex: sensing nutrient signals for autophagy activation. *Autophagy* 2013; 9:124-37; PMID:23295650; <http://dx.doi.org/10.4161/auto.23323>
- [40] Sinha RA, Singh BK, Zhou J, Wu Y, Farah BL, Ohba K, Lesmana R, Gooding J, Bay BH, Yen PM. Thyroid hormone induction of mitochondrial activity is coupled to mitophagy via ROS-AMPK-ULK1 signaling. *Autophagy* 2015; 11:1341-57; PMID:26103054; <http://dx.doi.org/10.1080/15548627.2015.1061849>
- [41] Egan DF, Shackelford DB, Mihaylova MM, Gelino S, Kohnz RA, Mair W, Vasquez DS, Joshi A, Gwinn DM, Taylor R, et al. Phosphorylation of ULK1 (hATG1) by AMP-activated protein kinase connects energy sensing to mitophagy. *Science* 2011; 331:456-61; PMID:21205641; <http://dx.doi.org/10.1126/science.1196371>
- [42] Xing J, Liu H, Yang H, Chen R, Chen Y, Xu J. Upregulation of Unc-51-like kinase 1 by nitric oxide stabilizes SIRT1, independent of autophagy. *PLoS One* 2014; 9:e116165; PMID:25541949; <http://dx.doi.org/10.1371/journal.pone.0116165>
- [43] Konno H, Konno K, Barber GN. Cyclic dinucleotides trigger ULK1 (ATG1) phosphorylation of STING to prevent sustained innate immune signaling. *Cell* 2013; 155:688-98; PMID:24119841; <http://dx.doi.org/10.1016/j.cell.2013.09.049>
- [44] Joshi A, Iyengar R, Joo JH, Li-Harms XJ, Wright C, Marino R, Winbrom BJ, Phillips A, Temirov J, Sciarretta S, et al. Nuclear ULK1 promotes cell death in response to oxidative stress through PARP1. *Cell Death Differ* 2015; 23:216-30; PMID:26138443
- [45] Rajesh S, Bago R, Odintsova E, Muratov G, Baldwin G, Sridhar P, Rajesh S, Overduin M, Berditchevski F. Binding to syntenin-1 protein defines a new mode of ubiquitin-based interactions regulated by phosphorylation. *J Biol Chem* 2011; 286:39606-14; PMID:21949238; <http://dx.doi.org/10.1074/jbc.M111.262402>
- [46] Oosterveer MH, Grefhorst A, Groen AK, Kuipers F. The liver X receptor: control of cellular lipid homeostasis and beyond Implications for drug design. *Prog Lipid Res* 2010; 49:343-52; PMID:20363253; <http://dx.doi.org/10.1016/j.plipres.2010.03.002>
- [47] Chan EY, Longatti A, McKnight NC, Tooze SA. Kinase-inactivated ULK proteins inhibit autophagy via their conserved C-terminal domains using an Atg13-independent mechanism. *Mol Cell Biol* 2009; 29:157-71; PMID:18936157; <http://dx.doi.org/10.1128/MCB.01082-08>
- [48] Petherick KJ, Conway OJ, Mpamhanga C, Osborne SA, Kamal A, Saxty B, Ganley IG. Pharmacological inhibition of ULK1 kinase blocks mammalian target of rapamycin (mTOR)-dependent autophagy. *J Biol Chem* 2015; 290:11376-83; PMID:25833948; <http://dx.doi.org/10.1074/jbc.C114.627778>
- [49] Dunlop EA, Hunt DK, Acosta-Jaquez HA, Fingar DC, Tee AR. ULK1 inhibits mTORC1 signaling, promotes multisite Raptor phosphorylation and hinders substrate binding. *Autophagy* 2011; 7:737-47; PMID:21460630; <http://dx.doi.org/10.4161/auto.7.7.15491>
- [50] Lee SB, Kim S, Lee J, Park J, Lee G, Kim Y, Kim JM, Chung J. ATG1, an autophagy regulator, inhibits cell growth by negatively regulating S6 kinase. *EMBO Rep* 2007; 8:360-5; PMID:17347671; <http://dx.doi.org/10.1038/sj.embor.7400917>
- [51] Jung CH, Seo M, Otto NM, Kim DH. ULK1 inhibits the kinase activity of mTORC1 and cell proliferation. *Autophagy* 2011; 7:1212-21; PMID:21795849; <http://dx.doi.org/10.4161/auto.7.10.16660>
- [52] Kim K, Pyo S, Um SH. S6 kinase 2 deficiency enhances ketone body production and increases peroxisome proliferator-activated receptor α activity in the liver. *Hepatology* 2012; 55:1727-37; PMID:22183976; <http://dx.doi.org/10.1002/hep.25537>
- [53] Sengupta S, Peterson TR, Laplante M, Oh S, Sabatini DM. mTORC1 controls fasting-induced ketogenesis and its modulation by ageing. *Nature* 2010; 468:1100-4; PMID:21179166; <http://dx.doi.org/10.1038/nature09584>
- [54] Albers M, Blume B, Schlueter T, Wright MB, Kober I, Kremoser C, Deuschle U, Koegl M. A novel principle for partial agonism of liver X receptor ligands. Competitive recruitment of activators and repressors. *J Biol Chem* 2006; 281:4920-30; PMID:16354658; <http://dx.doi.org/10.1074/jbc.M510101200>
- [55] Phelan CA, Weaver JM, Steger DJ, Joshi S, Maslany JT, Collins JL, Zuercher WJ, Willson TM, Walker M, Jaye M, et al. Selective partial agonism of liver X receptor α is related to differential corepressor recruitment. *Mol Endocrinol* 2008; 22:2241-9; PMID:18669643; <http://dx.doi.org/10.1210/me.2008-0041>
- [56] Yamaguchi K, Yang L, McCall S, Huang J, Yu XX, Pandey SK, Bhanot S, Monia BP, Li YX, Diehl AM. Inhibiting triglyceride synthesis improves hepatic steatosis but exacerbates liver damage and fibrosis in obese mice with nonalcoholic steatohepatitis. *Hepatology* 2007; 45:1366-74; PMID:17476695; <http://dx.doi.org/10.1002/hep.21655>
- [57] Bailey AP, Koster G, Guillemer C, Hirst EM, MacRae JI, Lechene CP, Postle AD, Gould AP. Antioxidant Role for Lipid Droplets in a Stem Cell Niche of *Drosophila*. *Cell* 2015; 163:340-53; PMID:26451484; <http://dx.doi.org/10.1016/j.cell.2015.09.020>

- [58] Park HW, Park H, Semple IA, Jang I, Ro SH, Kim M, Cazares VA, Stuenkel EL, Kim JJ, Kim JS, et al. Pharmacological correction of obesity-induced autophagy arrest using calcium channel blockers. *Nat Commun* 2014; 5:4834; PMID:25189398; <http://dx.doi.org/10.1038/ncomms5834>
- [59] Inami Y, Yamashina S, Izumi K, Ueno T, Tanida I, Ikejima K, Watanabe S. Hepatic steatosis inhibits autophagic proteolysis via impairment of autophagosomal acidification and cathepsin expression. *Biochem Biophys Res Commun* 2011; 412:618-25; PMID:21856284; <http://dx.doi.org/10.1016/j.bbrc.2011.08.012>
- [60] Kashima J, Shintani-Ishida K, Nakajima M, Maeda H, Unuma K, Uchiyama Y, Yoshida K. Immunohistochemical study of the autophagy marker microtubule-associated protein 1 light chain 3 in normal and steatotic human livers. *Hepatol Res* 2013; PMID:23773367
- [61] Gonzalez-Rodriguez A, Mayoral R, Agra N, Valdecantos MP, Pardo V, Miquilena-Colina ME, Vargas-Castrillón J, Lo Iacono O, Corazzari M, Fimia GM, et al. Impaired autophagic flux is associated with increased endoplasmic reticulum stress during the development of NAFLD. *Cell Death Dis* 2014; 5:e1179; PMID:24743734; <http://dx.doi.org/10.1038/cddis.2014.162>
- [62] Las G, Serada SB, Wikstrom JD, Twig G, Shirihai OS. Fatty acids suppress autophagic turnover in β -cells. *J Biol Chem* 2011; 286:42534-44; PMID:21859708; <http://dx.doi.org/10.1074/jbc.M111.242412>
- [63] Kovsan J, Bluhner M, Tarnowski T, Kloting N, Kirshtein B, Madar L, Shai I, Golan R, Harman-Boehm I, Schön MR, et al. Altered autophagy in human adipose tissues in obesity. *J Clin Endocrinol Metab* 2011; 96:E268-77; PMID:21047928; <http://dx.doi.org/10.1210/jc.2010-1681>
- [64] Lake AD, Novak P, Hardwick RN, Flores-Keown B, Zhao F, Klimecki WT, Cherrington NJ. The adaptive endoplasmic reticulum stress response to lipotoxicity in progressive human nonalcoholic fatty liver disease. *Toxicol Sci* 2014; 137:26-35; PMID:24097666; <http://dx.doi.org/10.1093/toxsci/kft230>
- [65] Portovedo M, Ignacio-Souza LM, Bombassaro B, Coope A, Reginato A, Razolli DS, Torsoni MA, Torsoni AS, Leal RF, Velloso LA, et al. Saturated fatty acids modulate autophagy's proteins in the hypothalamus. *PLoS One* 2015; 10:e0119850; PMID:25786112; <http://dx.doi.org/10.1371/journal.pone.0119850>
- [66] Martinet W, De Meyer GR, Andries L, Herman AG, Kockx MM. In situ detection of starvation-induced autophagy. *J Histochem Cytochem* 2006; 54:85-96; PMID:16148314; <http://dx.doi.org/10.1369/jhc.5A6743.2005>
- [67] Dupont N, Chauhan S, Arko-Mensah J, Castillo EF, Masedunskas A, Weigert R, Robenek H, Proikas-Cezanne T, Deretic V. Neutral lipid stores and lipase PNPLA5 contribute to autophagosome biogenesis. *Curr Biol* 2014; 24:609-20; PMID:24613307; <http://dx.doi.org/10.1016/j.cub.2014.02.008>
- [68] Shpilka T, Welter E, Borovsky N, Amar N, Mari M, Reggiori F, Elazar Z. Lipid droplets and their component triglycerides and sterol esters regulate autophagosome biogenesis. *EMBO J* 2015; 34:2117-31; PMID:26162625; <http://dx.doi.org/10.15252/embj.201490315>
- [69] Ogasawara Y, Itakura E, Kono N, Mizushima N, Arai H, Nara A, Mizukami T, Yamamoto A. Stearoyl-CoA desaturase 1 activity is required for autophagosome formation. *J Biol Chem* 2014; 289:23938-50; PMID:25023287; <http://dx.doi.org/10.1074/jbc.M114.591065>
- [70] Bestebroer J, V'Kovski P, Mauthe M, Reggiori F. Hidden behind autophagy: the unconventional roles of ATG proteins. *Traffic* 2013; 14:1029-41; PMID:23837619; <http://dx.doi.org/10.1111/tra.12091>
- [71] Madeira JB, Masuda CA, Maya-Monteiro CM, Matos GS, Montero-Lomeli M, Bozaquel-Morais BL. TORC1 inhibition induces lipid droplet replenishment in yeast. *Mol Cell Biol* 2015; 35:737-46; PMID:25512609; <http://dx.doi.org/10.1128/MCB.01314-14>
- [72] Li D, Song JZ, Li H, Shan MH, Liang Y, Zhu J, Xie Z. Storage lipid synthesis is necessary for autophagy induced by nitrogen starvation. *FEBS Lett* 2015; 589:269-76; PMID:25500271; <http://dx.doi.org/10.1016/j.febslet.2014.11.050>
- [73] Shpilka T, Elazar Z. Lipid droplets regulate autophagosome biogenesis. *Autophagy* 2015; 11:2130-1; PMID:26513372
- [74] Pardo V, Gonzalez-Rodriguez A, Muntane J, Kozma SC, Valverde AM. Role of hepatocyte S6K1 in palmitic acid-induced endoplasmic reticulum stress, lipotoxicity, insulin resistance and in oleic acid-induced protection. *Food Chem Toxicol* 2015; 80:298-309; PMID:25846498; <http://dx.doi.org/10.1016/j.fct.2015.03.029>
- [75] Bae EJ, Xu J, Oh DY, Bandyopadhyay G, Lagakos WS, Keshwani M, Olefsky JM. Liver-specific p70 S6 kinase depletion protects against hepatic steatosis and systemic insulin resistance. *J Biol Chem* 2012; 287:18769-80; PMID:22493495; <http://dx.doi.org/10.1074/jbc.M112.365544>
- [76] Watson PJ, Fairall L, Schwabe JW. Nuclear hormone receptor co-repressors: structure and function. *Mol Cell Endocrinol* 2012; 348:440-9; PMID:21925568; <http://dx.doi.org/10.1016/j.mce.2011.08.033>
- [77] Baldan A, Bojanic DD, Edwards PA. The ABCs of sterol transport. *J Lipid Res* 2009; 50 Suppl:S80-5; PMID:18997165
- [78] Wagner BL, Valledor AF, Shao G, Daige CL, Bischoff ED, Petrowski M, Jepsen K, Baek SH, Heyman RA, Rosenfeld MG, et al. Promoter-specific roles for liver X receptor/corepressor complexes in the regulation of ABCA1 and SREBP1 gene expression. *Mol Cell Biol* 2003; 23:5780-9; PMID:12897148; <http://dx.doi.org/10.1128/MCB.23.16.5780-5789.2003>
- [79] Xu J, Ji J, Yan XH. Cross-talk between AMPK and mTOR in regulating energy balance. *Crit Rev Food Sci Nutr* 2012; 52:373-81; PMID:22369257; <http://dx.doi.org/10.1080/10408398.2010.500245>
- [80] Severgnini M, Sherman J, Sehgal A, Jayaprakash NK, Aubin J, Wang G, Zhang L, Peng CG, Yucius K, Butler J, et al. A rapid two-step method for isolation of functional primary mouse hepatocytes: cell characterization and asialoglycoprotein receptor based assay development. *Cytotechnology* 2012; 64:187-95; PMID:22105762; <http://dx.doi.org/10.1007/s10616-011-9407-0>